FAST NEGATIVE HYDROGEN IONS

by

A. Charles Whittier

A thesis submitted to the Faculty
of Graduate Studies and Research
of McGill University, in partial
fulfilment of the requirements for
the degree of Doctor of Philosophy

Radiation Laboratory

August, 1952

TABLE OF CONTENTS

DIAGRAMS AND PLATES

Page

Diagrams

Page

Plates

SUMMARY

Protons were directed through hydrogen gas and were found to capture electrons to form negative hydrogen ions. When sufficient gas had been traversed, the ratio of negative ions to protons reached an equilibrium value which was a maximum of 22.2 percent at about 8.5 kilovolts. The energy interval investigated was from 4 to 70 kilovolts. In this interval, the electron loss cross-section for the negative hydrogen ion was determined. It varied from 6.3×10^{-16} cm.^{2} at 4.2 kilovolts, to 2.5×10^{-16} cm.^{2} at 70.3 kilovolts. A calculation of the electron capture cross-section for the neutral hydrogen atom in the same energy interval was made. A determination of the electron capture cross-section for protons between the above mentioned energies was also made, and found to agree with values obtained by other workers, both theoretical and experimental.

A seven stage voltage-multiplier circuit operated at radio-frequency, an ion accelerator and analyser were designed for this work and are described.

ACKNOWLEDGMENTS

The author wishes to express his thanks to Professor J.S. Foster for extending the facilities of the Radiation Laboratory for the research, and to Professor F.R. Terroux for his help and encouragement as the director of the research. Thanks are also due to Professor J.D. Jackson for many helpful discussions and calculations regarding the theoretical side of the experiment, to Dr. D.E. Tilley for helpful suggestions, to Mr. F.S. Eadie for the loan of equipment, and to Messrs S. Doig and R. Lorimer for their invaluable help in the construction of the apparatus. The author also acknowledges a Scholarship from the Ontario Research Council, and a Studentship from the National Research Council of Canada.

INTRODUCTION

Negative ions of hydrogen have been observed under various experimental conditions, and have been studied to a greater extent theoretically. However these ions have been the subject of very little experimental research of a quantitative nature.

In 1936 O. Tuxen drew negative ions from a hydrogen discharge and analysed them with a mass spectrograph (1). He was able to show that these ions were truly H^- and did not arise from OH or other atomic or molecular combinations. Hylleraas had already shown by wave mechanical analysis that H^- could exist and that the electron affinity would be $0.70 \pm .015$ ev. (2). This has not been verified experimentally.

The fact that H^- existed had an interesting application in the explanation of the variation of the continuous emission spectrum of the sun between 4,000 and 12,000 A^o. The suggestion was made by Wildt that the absorption of radiation in this wavelength region was caused by negative hydrogen ions in the sun's photosphere (3). This was quantitatively verified by A.J. Deutsch who was able to obtain a theoretical absorption spectrum of H^- which corresponded to the observed absorption of the solar radiation (4). It is to be pointed out that no corresponding emission spectrum of H^- has ever been observed in the laboratory; this is understandable considering that the spectrum is continuous, and that the probability of radiative capture of an electron by a neutral hydrogen atom is quite low (19).

Most wave mechanical studies of the negative hydrogen ion showed that only one stable state existed. These calculations have been carried out by a number of people (5 - 12). Recently however, Hylleraas has predicted a second energy state of H^- with an electron affinity of 0.29 ev. (13), but points out that it is unstable against auto-ionization. This too has yet

to be verified by experimental observation.

The first observation of positive hydrogen ions capturing electrons to produce negative hydrogen ions was made in 1936 by Arnot and Milligan when they bombarded a nickel surface with the positive ions (14). Several other investigations of this phenomenon have been made (15), (16).

In 1951 Lofgren obtained photographic evidence of the existence of negative hydrogen ions in the 184-inch Berkeley synchrocyclotron (17). A photographic plate was placed in such a way that it would detect particles originating from the small orbits near the centre of the accelerator. Two bands of particles were observed; one was due to particles leaving the ordinary proton orbits tangentially, the other was due to particles leaving counter rotating orbits the same way. These bands were identified as being due to neutral hydrogen atoms and negative hydrogen ions respectively. The particles had energies of several Mev.

The only quantitative experimental measurements of the properties of H^- so far, were carried out by J.B. Hasted (18). A Nier type ion source, in which hydrogen was bombarded by electrons and the resultant negative hydrogen ions forced out by electrostatic repulsion, was used to produce H^- ions. These ions were focussed to a beam and fired through a gaseous target. The electron loss cross-sections for H^- in the noble gases Xe, Kr, A, Ne, and He were measured at energies ranging from about 100 to about 3,000 ev. In this energy range the loss cross-section, in all cases, increased steadily with energy. In the case of H^- through He, the cross-section increased from about 2×10^{-16} cm.^{2} at 100 ev. to about 3×10^{-16} cm.^{2} at 1700 ev., the maximum energy used in this case.

On the theoretical side, only the radiative capture cross-section has been calculated. The absorption cross-section, Q_a, of H^- has been determined

(19) for the process

$$H^- + h\nu \rightarrow H + e^-$$

Then by using the relation

$$Q_c = \frac{h\nu}{m^2v^2c^2}\frac{g^-}{g^o}Q_a$$

where m and v relate to the mass and velocity of an electron incident on a neutral hydrogen atom, c the velocity of light, ν the frequency of the absorbed radiation, g^- and g^o are the statistical weights of the ground states of H^- and of the neutral hydrogen atom, the radiative capture cross-section (Q_c) was determined (22). Where electron energies ranged from .14 to 7 ev. the value of Q_c was of order 10^{-22} cm.^{2}

Negative ions can be formed in a variety of ways (20). A neutral hydrogen atom passing through a gas can capture a free electron with the excess energy being carried off by radiation. The emission spectrum will be continuous if only one bound state exists. If a neutral atom captures a bound electron from a gas atom, we have a three body process in which the ionized gas atom, the third body, can carry off the excess energy, and there is no radiation emitted.

A further process has been proposed by Massey based on the Franck-Condon principle (20). According to this principle an excited hydrogen molecule dissociates into a negative and a positive ion. Of course several things can happen, but for certain atomic separations and degrees of excitation, negative ions can be formed in preference to de-excitation with radiation, or straight dissociation into two neutral atoms. This process of H^- production probably accounts for the presence of H^- in gaseous discharges, and in the ion source used by Hasted (18). It is unfortunate that Keene (21) who fired a proton beam through hydrogen and analysed the mass spectrum of positive gaseous ions left in the beam path, did not do a similar analysis

of the negative ions left behind, as such an analysis could have shed light on the probability of the Franck-Condon process actually taking place.

As has also been noted, positive ions impinging on metallic surfaces can form negative ions. It is probable that atoms, excited atoms, and positive ions can all capture electrons from metal surfaces to form H^- (22).

It has been suggested, although the origin of the suggestion is unknown to the author, that the effective accelerating potential of an ion accelerator could be doubled by the use of negative ions. Thus, suppose that the maximum available voltage were + E kv. and that there were a suitable source of H^- at or near ground potential. Then the negative ions could be focussed into a beam, accelerated to + E kv and fired through a thin barrier such as a foil or gas chamber. The electrons would then be stripped from the particles by the stationary atoms in the barrier, and we would have a supply of protons of energy E kv, at a potential of +E kv. These could then be accelerated through E kv again, impinging on a target at ground potential. Thus the final proton energy would be 2E kv. A further advantage would be that both the ion source and the target would be at ground potential, with a great simplification of insulation problems. Although Hasted employed a Nier type ion source for obtaining H^- ions, no figures were given regarding the H^- beam intensity. There are several types of positive ion sources from which copious supplies of protons can be obtained (31). If a simple, yet efficient method of converting positive into negative ions were available, the double acceleration process with high intensity beams might be possible. The findings of the present research might be of use in designing such an H^- source and accelerator.

A considerable amount of investigation has been directed toward determining the probability of a proton capturing or a neutral atom losing an electron as a beam of hydrogen particles passes through a gas (22). It is pertinent to the present investigation to discuss briefly the methods used.

In the investigations of Goldman a beam of protons was directed through a gas chamber (23). Some of the protons captured electrons to form neutral atoms. Those protons which did not capture electrons were detected after the beam had emerged from the chamber. The gas pressure was kept low enough that the neutral atoms once formed had little chance of being re-ionized. From the observations of the variation of charged beam absorption with pressure, the electron capture cross-section for the proton was calculated, for incident proton energies ranging from 500 to 4,000 ev. Smith used this method for proton energies from 1300 to 8,000 ev. (42). This has been called the beam absorption method, although it is to be noted that few if any particles are actually absorbed by the gas, but rather that some of the particles lose their charge and hence are not detected. In this and other experiments loss of beam particles by gas scattering was shown to be so small as to have a negligible effect on the results.

Bartels used what might be called an equilibrium beam concentration method (24). A proton beam was passed through hydrogen gas, the pressure of which could be varied. The charged particles in the beam which had emerged from the gas could be deflected from the beam path by a system of electrostatic deflection plates and thus prevented from entering an ionization chamber which could detect uncharged as well as charged particles. By simultaneous measurements of the total beam, and of the neutral component of the beam, as functions of gas pressure, Bartels calculated the ratio of

charged to neutral particles, which, assuming no negative ion formation, gave H^+/H^o. For low pressures this ratio was quite high, but as the pressure was increased, the ratio fell and reached a final or equilibrium value at a pressure of about 10^{-2} mm. Hg. Calling the equilibrium ratio w, and the length of the beam path in the gas chamber x, then the mean free path λ for the capture of an electron, was given by the Wien formula (25),

$$\frac{1}{\lambda}(1 - w) = \frac{1}{x} \ell n \frac{(H^+/H^o)_p + 1}{(H^+/H^o)_p - w}$$

where $(H^+/H^o)_p$ is the value of the ratio for the gas pressure p concerned. The electron capture cross-section σ could be determined from λ since the cross-section is merely the reciprocal of the product of the mean free path and the number of gas atoms per c.c. at pressure p. That is

$$\sigma = 1/\lambda n$$

Bartels' measurements extended from about 5 to 35 kilovolts. Variations of this method have been used by other investigators to measure the capture cross-sections (26).

The most extensively used method is one in which a proton beam passes through a gas and ionizes it, and the number of ionized gas atoms and free electrons left in the path of the beam measured. The work of Keene is a good example of this method (27). A proton beam passed through a gas filled region between two plane parallel deflection plates. The gas atoms and molecules were ionized by the beam and the electrons either captured by the protons in the beam or left in the free state. Either negative or positive voltages could be applied to one of the deflection plates; the other plate was held at ground potential. Any ion current to the former plate could be measured by a d-c amplifier. By applying a voltage of the proper polarity to that plate, either the positive ions or the electrons left in the path

of the beam could be collected by it. The pertinent equations are,

$$I_+ = I_0 nL\ (\sigma_{c'} + \sigma_i)$$

$$I_- = I_0 nL\, \sigma_i$$

where I_0 is the incident proton current, I_+ and I_- the positive ion and electron currents to the collector plate, n the number of gas atoms per c.c., and L the length of the beam path between the deflection plates. The cross-section $\sigma_{c'}$ is that for a proton capturing an electron; σ_i is the cross-section for a proton to ionize the gas and leave a free electron. Other investigations employing the same method are listed in references (28) and (18).

Perhaps the most direct method of investigating the charge exchange of protons and neutral hydrogen atoms was used by Montague (29) and Ribe (30). Montague directed a beam of neutral hydrogen atoms through a gas chamber situated in a magnetic field. A special detector in the path of the beam detected neutral particles. As the gas pressure was raised an increasing amount of the neutral atomic beam became ionized, was deflected out of the beam path by the magnetic field, and so failed to enter the detector. A study of the reduction in neutral beam strength as a function of gas pressure gave a measure of the electron loss cross-section for the neutral hydrogen atom. Ribe, using the same apparatus, directed a beam of protons into the chamber. At the end of the curved ion path a Faraday cylinder was placed. Protons capturing electrons from the gas left the curved path tangentially and failed to enter the detector. Again, by plotting the detector current against pressure, the proton capture cross-section was determined.

Some of the values of the electron capture cross-sections for protons have been plotted as a function of incident proton energy in Fig. (1). The existence of rather large inconsistencies is evident even after consideration

has been given to the limits of accuracy placed on the values by those making the measurements.

Only in Ribe's paper was any mention made of the possibility of the occurrence of negative ions contributing to the error involved in making cross-section measurements (30). A beam of hydrogen ions was directed through an aluminized zapon foil and the ratio of H^- to protons in the emergent beam was measured. It was found that for an incident energy of 35 kv the ratio (H^-/H^+) was about 3 percent, while at 90 kv it was less than 0.1 percent. In the calculations of the cross-sections from observations with the method of Bartels, the equilibrium beam concentration method, no consideration was mentioned regarding the possibility of H^- formation. It seemed possible in the light of Ribe's spot measurements that the abnormally high values of capture cross-section at low energies as obtained by Bartels might possibly have been caused by negative hydrogen ions.

With the foregoing in mind, it was proposed to determine the extent to which protons, passing through hydrogen gas, capture electrons to form H^-, and to study the cross-sections relating to this process. It was found that reasonably consistent results for the electron capture cross-section for protons could also be obtained. It will be seen from Fig. (1) that the results obtained by previous investigators cover in most cases comparatively restricted limits of proton beam energy. It was therefore considered useful to cover the entire range from 4 to 70 kv by the method here described. The values so obtained have been included in Fig. (1).

THEORY

It will facilitate an understanding of the following discussion if reference is made to Fig. (2). Consider a beam of protons entering the Ion Exchange Chamber through a small aperture (A) which isolates the chamber from the ion accelerator. The pressure in this chamber will be referred to as p_i. The protons in the beam will capture electrons from the gas molecules to form neutral atoms. The neutral atoms can then either lose their electrons or capture more electrons in further collisions with the gas molecules. If the gas density is high enough the concentrations of neutral, positive, and negative particles will come into equilibrium with each other.

The electron capture cross-section (σ_c) for a proton passing through a given gas (sometimes called the charge exchange cross-section) may be thought of as the actual area presented by the atoms of the given gas to the incident beam for this process to take place. It should be obvious that it is a measure of the probability of electron capture occurring, and that the concept of area is instituted purely for simplicity of calculation. Similar definitions can be stated for the loss cross-section (σ_l) for a neutral atom, the electron capture cross-section (σ_c) for a neutral atom, and the electron loss cross-section (σ_l) for a negative ion. The differential equations relating to the charge exchange processes described are,

$$(1) \quad dH^+ = H^0 \, n \, \sigma_l \, dx - H^+ \, n \, \sigma_c \, dx$$

$$(2) \quad dH^- = H^0 \, n \, \sigma_c \, dx - H^- \, n \, \sigma_l \, dx$$

$$(3) \quad I = H^+ + H^- + H^0$$

where I is the intensity of the incident proton beam, H^+, H^-, and H^0 the intensities of protons, negative ions, and neutral atoms in the beam at a distance x from the entrance aperture (A), and n is the number of gas atoms per c.c.

When the beam components have reached equilibrium, and hence $dH^+ = dH^- = 0$, then from equation (1)

$$(4) \qquad \left(\frac{H^-}{H^0}\right)_e = \frac{\sigma_{c'}}{\sigma_{\ell'}}$$

and from equation (2)

$$(5) \qquad \left(\frac{H^-}{H^0}\right)_e = \frac{\sigma_c}{\sigma_\ell}$$

where the subscript "e" refers to equilibrium conditions.

Dividing (5) by (4) gives

$$(6) \qquad \left(\frac{H^-}{H^+}\right)_e = \frac{\sigma_c}{\sigma_\ell}\frac{\sigma_{c'}}{\sigma_{\ell'}}$$

Consider now the mixed beam leaving the Ion Exchange Chamber and entering the Observation Chamber, through aperture (B), where there is a transverse magnetic field and gas at pressure p_o. The beam will be analysed into components H^+, H^-, and H^o. Now consider two identical detectors placed so that one will pick up the negative component, and the other the positive component. The detector positions should be such that the length of the curved path of a proton from (B) to the positive ion detector be the same as the path distance for a negative ion of the same energy, from (B) to the negative ion detector. Thus if p_i is high enough, and p_o low enough, the value of $(H^-/H^+)_e$ can be measured directly.

If the pressure p_o is raised (p_i being held constant), some of the ions will, on interaction with the gas molecules, lose their charge and leave their curved paths; hence they will not enter the detectors.

The differential decrease in the negative ion beam travelling a distance dy through a gas of density n atoms per c.c. is

$$(7) \qquad dH^- = -H^- n \sigma_\ell \, dy$$

where y is distance measured along the ion path from (B). Thus the current to the negative ion detector is given by

$$(8) \qquad \ln H^- = n\sigma_\ell d + \text{constant.}$$

where "d" is the path distance from (B) to the detector. Since $n = kp_o$, where $k = \frac{1.93 \times 10^{16}}{T}$ for p_o measured in units of 10^{-3} mm. Hg, (T being the absolute temperature), then

$$(9) \qquad \ln H^- = -k p_o \sigma_l d + \text{const.}$$

Thus by determining H^- for various values of p_o, plotting a curve of ln H^- vs. p_o, and measuring the slope of the curve, the electron loss cross-section is given by,

$$(10) \qquad \sigma_l = -\frac{s_-}{kd}$$

where s_- is the slope value.

By a similar argument for the positive component of the beam

$$(11) \qquad \ln H^+ = -k p_o \sigma_{c'} d + \text{const.}$$

From this last relation it is obvious that if ln H^+ were plotted against p_o, and the slope of the curve designated s_+, then,

$$\sigma_{c'} = -\frac{s_+}{kd}$$

However for practical reasons, one of which was that p_o could not be kept low enough to measure $(H^-/H^+)_e$ directly, it was necessary to determine values of (H^-/H^+) as a function of p_o. Having obtained H^- and (H^-/H^+) for various pressures p_o, a separate measurement of H^+ would have been an extra and unnecessary observation. Thus the following indirect derivation of $\sigma_{c'}$ gives a relation which is best suited for the experimental determination of that cross-section.

Subtracting (11) from (9),

$$\ln\left(\frac{H^-}{H^+}\right) = \text{const.} - (\sigma_l - \sigma_{c'}) k p_o d$$

From the condition that at $p_o = 0$, $(H^-/H^+) = (H^-/H^+)_e$

$$\ln\left(\frac{H^-}{H^+}\right) = \ln\left(\frac{H^-}{H^+}\right)_e - (\sigma_l - \sigma_{c'}) k p_o d$$

Thus from a plot of $\ln (H^-/H^+)$ against p_o, one obtains $(H^-/H^+)_e$ from the ordinate intercept, and $(\sigma_l - \sigma_{c'})$ from the slope. That is,

$$(12) \qquad (\sigma_l - \sigma_{c'}) = -\frac{s_\mp}{kd}$$

where $s_{\mp}$ is the value of the slope of the curve $\ln (H^-/H^+)$ vs. p_o. Therefore

$$(13) \quad \sigma_{c'} = \sigma_{\ell} + \frac{s_{\mp}}{kd}$$

and from (10) and (13)

$$\sigma_{c'} = \frac{s_{\mp} - s_-}{kd}$$

Summarizing then, by obtaining a curve of $\ln H^-$ vs. p_o one can calculate σ_{ℓ}; a curve $\ln (H^-/H^+)$ vs. p_o will give $(H^-/H^+)_e$; and a combination of both curves will give $\sigma_{c'}$. Using known values of $\sigma_{\ell'}/\alpha'$, σ_c can be calculated from a rearrangement of equation (6),

$$\sigma_c = \sigma_{\ell} \left(\frac{H^-}{H^+}\right)_e \frac{\sigma_{\ell'}}{\sigma_{c'}}$$

It is to be noted that the method of obtaining $\sigma_{c'}$ just stated leaves a bit to be desired in that when $(s_{\mp} - s_-)$ becomes small in comparison to say $s_{\mp}$, very large errors in values for $\sigma_{c'}$ will result from relatively small errors in $s_{\mp}$. The primary object of the experiment was the measurement of $(H^-/H^+)_e$ and σ_{ℓ}, however it was found that reasonably acceptable results for $\sigma_{c'}$ could also be obtained by this method and so this further calculation was made and presented.

No direct measurements of $(H^+/H_o)_e$ or $(H^-/H_o)_e$ were made.

Solutions to the differential equations (1) and (2) have been given and discussed in Appendix I.

EXPERIMENTAL APPARATUS

The ion beam was obtained from an ion accelerator of the Cockcroft-Walton type (32). The source of positive ions was a hydrogen discharge tube; some of the ions in the positive plasma of the discharge drifted out of the source through a small opening, and into the accelerator tube. These ions were focussed into a beam and accelerated down the accelerator tube to the gaseous target. In addition to protons, emerging from the source, there were the molecular ions H_2^+ and H_3^+. The experimental chambers at the bottom of the accelerator have been briefly outlined in the section on Theory.

Details of the apparatus used in this experiment will be discussed in what follows.

Ion Source

The hydrogen ions were produced in a pyrex capillary arc type ion source designed after Lamar, Buechner, and Van de Graaf (33). Details of construction are shown in Fig. (3). The plate and cathode bulbs were joined by a pyrex tube, termed the capillary, 2.5 cm. long and 0.4 cm. inside diameter. A small conical hole was ground into the side of the capillary in such a way that the inner end of the hole had zero thickness. The inner end of this hole had a diameter of 0.5 mm. The plate and cathode leads were held in position through ground glass joints fitted to the bulbs as shown. The focussing cone was machined from a copper block in the top of which was a semi-cylindrical groove. The capillary sat in this groove with about .005 inch clearance on the radius. The diameter of the hole at the top of the copper block was made the same size as the large diameter of the conical hole in the side of the glass capillary so that when the pyrex tube and the copper block were assembled the complete outlet cone was smooth from the inside of the capillary right down to the bottom of the copper block. The

outside of the capillary was platinized and copper plated with a thin copper coat. The plating process was done by immersing the platinized capillary into a solution of 200 g/l of $CuSO_4$ and 75 g/l of H_2SO_4, and running a current of 60 ma per cm^2. for about two minutes. The plated capillary was then set into the groove on the block, care being taken that the two cones coincided, and the assembly soft soldered together. This gave a fairly strong, vacuum tight joint which caused no trouble in spite of the fact that the capillary temperature rose for short periods as high as 70°C. during operation. For normal operation the joint temperature was not allowed to rise more than 10°C. above room temperature; cooling was effected by a jet of compressed air.

A directly heated cathode was used. An eight centimeter length of the filament ribbon* used in 866 rectifier tubes was shaped as shown in Fig. (3). It was spot welded to the two tungsten leads sealed in the female ground joint. The filament was dipped into a radio solution R-500** and allowed to dry.

The plate from a discarded 8016 rectifier was modified and spot welded to the tungsten lead through the other female ground joint, to form the plate of the ion source.

Silicone high vacuum grease was used on the ground joints.

Hydrogen was introduced to the source through a flat ribbon type adjustable slow leak.

Plate voltage was supplied by a motor generator set which would produce 110 volts d.c. A 1/4 h.p. a.c. motor drove the generator through a 1/2 inch

* Courtesy of R.C.A., Harrison, N.J.

** Courtesy of Baker Chemica Co., Phillipsburg, Pa.

bakelite shaft eight inches long. Filament power (3 volts, 5.5 amps.) was obtained from storage batteries. The electrical system for the ion source was mounted on bakelite boards secured to a wooden stand. Fig. (4) shows the wiring diagram.

Before the arc could be operated properly the filament had to be activated. The filament was heated to about 1100° C. by a filament voltage of 3 volts for approximately 45 minutes; during this time large volumes of gas were given off by the coating. Hydrogen was then admitted to the source at operating pressure. The plate voltage was turned on and the arc started with the assistance of a spark coil electrode applied to the glass envelope of the source. The filament voltage was then taken up to about 4.5 volts (1350° C.) for 15 or 20 seconds during which time the emission increased considerably. The filament voltage was then reduced to 3 volts; the emission dropped by a few percent and then remained steady. Typical values for the arc were,

Plate voltage	90 volts
Plate current	0.2 amperes
Filament voltage	3 volts
Filament current	5.5 amperes.

No direct measurement of pressure in the ion source was made but from a consideration of the vacuum system pressure, pump speed, and source outlet area, the source pressure can be shown to have been between 0.1 and 0.15 mm Hg.

There were certain difficulties involved with this type of source. Several tubes had to be made before one that would give reliable operation was obtained. In general design they were the same, but in detail they differed. It was found that in order to keep the plate dissipation to a

minimum the plate voltage had to be low; and in order to keep the pressure in the high vacuum system of the accelerator tube to less than 3×10^{-4} mm. Hg the source had to operate at a pressure lower than a certain maximum. Some sources tried had too high a plate voltage, too high a pressure, or both. There was no obvious relation between geometry, plate voltage, and pressure, but by varying the length and shape of the capillary a satisfactory discharge tube was finally obtained. It might be noted that in one tube, the ground outlet hole of which was copper plated, the arc would not strike. However when the plating was removed from the outlet hole, an arc could be started, but it was unstable. Sometimes the filament would sputter onto the glass walls; this seemed to help rather than hinder the operation of the arc.

Exposing an activated filament to the atmosphere did not seem to affect it in any way. In fact while one filament was at operating temperature, a breakage in the vacuum system allowed air into the ion source at atmospheric pressure; its subsequent operation did not seem to be impaired. However the lifetime of a filament was relatively short. Due to the capillary between the plate and the cathode the arc drop across the tube was necessarily much higher than would be the case were there no such constriction. Thus the positive ions in the plasma could be accelerated to quite high velocities before they struck the filament. When they did strike, they subjected the filament coating to a much more destructive bombardment than would have been the case in an ordinary gaseous rectifier where the arc drop is low. One filament lasted through most of the experiment, with a lifetime of about 100 hours.

Accelerator Tube

Positive ions drifting out of the ion source were collected, focussed, and accelerated by five cylindrical electrodes made of dural, arranged as shown in Fig. (5). In order that the fields in the gaps should have good symmetry and also that there should be no sharp points allowing corona discharges, rings were machined on the ends of the electrodes. The inside diameter of the smaller electrodes was 3/4 inches, that of the larger ones about 1 1/2 inches. The distance from the focussing cone of the ion source to the first electrode was 1/4 inch; the next gap was 3/8 inches, and the remaining gaps were 1/2 inches. Except for the second electrode, each was turned out in one piece; the second electrode was made by snug fitting a smaller part to the larger part. Each electrode was held in place, by a system of clamps and adjustment screws, to a flat 1/8 inch thick dural ring. As shown in the diagram the sections were spaced by glass cylinders 4 inches in diameter.

The electrodes were machined with a .001 inch tolerance on inner radius so that they could be properly aligned by a rod accurately positioned at the bottom of the tube and running up its full length. This alignment rod was first bolted to the base of the tube. The electrodes were slid over the rod and clamped in position to the rings as the tube was built up, a section at a time. The rod was then carefully withdrawn.

The vacuum seals between the glass cylinders and the metal rings were made with Apiezon "Q" compound. These seals gave no trouble at any time.

A 3/8 inch thick brass plate topped the tube. A hole in the centre of this plate admitted the copper block of the ion source with a .002 inch radial clearance. A slight recess around the hole took a neoprene gasket

and the shoulder of the copper block as shown in Fig. (3).

The base of the tube was bolted firmly to the dural top of a steel mounting table.

At the bottom of the base were four screw holes around a 1 1/2 inch diameter hole so that any desired experimental apparatus could be accurately positioned. This arrangement also served to position the alignment rod during assembly of the accelerator tube. In one side of the base was a 1/4 inch copper tube leading to a McLeod Gauge; at the back was a 2 inch pumping manifold.

Connected to the pumping manifold by a ground glass joint was a glass tube of the same diameter as the manifold and ten inches in length, leading to a 20 litre per second oil diffusion pump. The forepump used was a 0.5 litre per second Megavac. It is worthy of note that although there was gas entering the accelerator tube continuously from both the ion source at the top of the column, and from the experimental apparatus at the bottom, evacuation from just the one manifold kept the pressure in the accelerator tube low enough to permit satisfactory operation.

When the gas inlets at the top and bottom of the tube were closed off, a pressure of 6×10^{-5} mm. Hg was obtained; with the ion source operating, and the experimental equipment at the bottom held at normal experimental pressures, the pressure in the accelerator was 2×10^{-4} mm. Hg.

High Voltage Supply

Accelerating potentials were obtained from a high voltage supply of the Cockcroft-Walton type operated at radio-frequency. The idea of using an r-f supply for an accelerator of this type had been suggested by Lorrain (34).

Radio-frequency high voltage supplies with output voltages as high as 50 kv d-c and using as many as two voltage-doubler stages had been in successful operation (35). As far as was known, however, no r-f supply had been constructed for higher output voltages, although circuits supplying up to 200 kv had been built which operated at frequencies of a few kilocycles (36). Lorrain had pointed out that the use of r-f would keep the ripple voltage at a very low level and that the circuit component would be relatively inexpensive and have small physical size. The decision to construct an r-f supply was based on two reasons: first because of the low cost, low ripple, and small size; second, to determine whether or not such a supply was as practical as suggested.

A block diagram of the high voltage supply is shown in Fig. (6).

A regulated 600 volt d-c power supply shown in Fig. (7) supplied plate voltage to an 807 beam power tube. A separate oscillator drove the grid of the 807 at the desired frequency; cf Fig. (8). The r-f power from the 807 was fed to a 10 kv r-f transformer through a suitable matching circuit. The high voltage r-f from the transformer was then applied to the Cockcroft-Walton voltage-multiplier circuit which consisted of seven voltage-doubler sections, shown in Fig. (9). Thus, a d-c voltage approximately 14 times the peak voltage on the secondary of the transformer was obtained at the output end of the multiplier circuit.

The condensers in the multiplier were 20 kv .001 $\mu\mu$f, the diodes 1B3/8016 high vacuum rectifiers. The r-f transformer was a commercial type with a 150 μh primary inductance, and a 42 mh secondary inductance. The secondary inductance shunted by the stray capacitance of the secondary circuit determined the frequency at which the greatest power could be supplied to the voltage-multiplier circuit. It was found that

the best results could be obtained only when the power tube was driven by a separate (and well shielded) oscillator. This is to be contrasted with the standard method of driving the 807 by a small feedback voltage from a tickler coil at the top of the r-f transformer. The use of a separate oscillator meant that the tube had to be matched to the transformer by a suitable matching circuit.

It was stated that one of the main advantages of using an r-f supply was that the ripple voltage on the output should be low. The ripple voltage is usually given by

$$\delta V = \frac{i}{4fc} n(n+1)$$

where i is the d-c load current, f the frequency, C the capacitance of each condenser, and n the number of doubling stages. Thus, according to this relation, the higher the frequency the lower the ripple. However this neglects to take into account the stray capacitance across the two branches of the circuit. When the circuit was completed it was found that there existed a large stray capacity. Measurements showed that an r-f current was being conducted through this stray capacity and then through the .001 μf condensers in such a way that it introduced a very large ripple on the d-c output - the very thing that the r-f was to eliminate. It had been suggested that inductances (with blocking condensers) of such a value as to resonate with the stray capacitances be placed across the rectifier tubes (34). This was ruled out on the grounds that the choke coils would absorb power, and hence further lower the performance of the circuit, and that the coils would have had to be very large physically. A satisfactory answer was found by placing an inductance, identical with the secondary of the r-f transformer, across

the last condenser of the circuit; i.e. at the output end of the multiplier. Although this decreased the effective inductance of the secondary circuit (it was in parallel with the secondary of the r-f transformer) and hence reduced the resonant frequency, it greatly improved the efficiency of the circuit and all but eliminated the ripple voltage. With a d-c output of 10 kv and load current of 42 μa the ripple voltage was measured with the added inductance, L_b, on and with it off; in the first case the ripple was 17 volts, in the second 250 volts r.m.s. The measurement of ripple at higher output voltages was not feasible. In Fig. (10) are shown the d-c voltages obtained at the various sections in the two cases. The blocking condenser C_b was necessary to keep d-c out of inductance L_b. As a further means of giving stability to the output, five 20 kv .001 μf condensers were put in series from the output point to ground; each condenser was tied into an appropriate point of the voltmeter bleeder resistor.

The 600 volt power supply and oscillator were built on chassis which were fitted into a control rack. The voltage-multiplier, r-f transformer, 807 tube and associated circuits were mounted together in a specially designed lucite box. The two units were connected with low power loss shielded cable. At each d-c point on the multiplier was an output terminal. The terminals were on the outside of the box and of such a shape as to make a fit with grid caps.

The body of the box, which contained the high potential circuit components, was filled with transformer oil, as indicated in Fig. (9). The tops of the diodes protruded through the lucite top of the box.

The high voltage circuit operated at a frequency of 102 kc.

Filament Power

Various methods have been suggested and used for supplying power to the diode filaments in a voltage multiplier circuit. These include using 1 1/2 volt dry cells, pickup from the r-f transformer by a wire loop, and pickup from the r-f circulating currents which have been conducted by the stray capacitances. For various reasons none of these methods seemed satisfactory for the present circuit.

A new method was tried; see Fig. (11). An oscillator fed power into a series of r-f isolating transformers; the primary of one transformer was connected across the secondary of the previous one along with a small variable condenser for tuning. Each transformer winding was wave wound by hand close to one end of a 1 inch diameter glass cylinder 3/4 inches long. When the windings were finished they were coated with polystyrene by dipping them into a solution of polystyrene and carbon tetrachloride. The primary and secondary of each transformer were separated by 1/4 inch with lucite spacers, and the whole assembly held firmly to the bottom of the lucite box by a long lucite bolt which screwed into a threaded hole in the bottom. Two loops of wire were placed around each transformer. Each loop picked up a small amount of power which was fed to a diode filament. Before the final arrangement was settled, several arrangements had to be tried; inductance values, frequency, coil spacing, size of pick-up loops, etc., were all varied. Due to the complexity of the circuit (from an analytical point of view) this trial and error method was probably the quickest way to design it. In the final circuit each transformer winding had an inductance of 240 μh. Each pick-up loop had one, two, or three turns depending on whether it was close to or far away from the input end of the circuit. The tuning condensers were 140 $\mu\mu$f variable air condensers.

The filament circuit was mounted in the lucite box with the other components of the voltage-multiplier circuit and so was oil immersed. For tuning purposes small 2.2 volt flashlight bulbs were connected to the tube sockets, and the circuit tuned until all bulbs had the same brightness as a similar one heated by a 1 1/2 volt dry cell. The bulbs were then removed and replaced by the 1B3/8016 rectifiers. Plate voltage for the oscillator tube, a 6Y6G, was obtained from a regulated 220 volt power supply. The filament circuit operated at a frequency of 1300 kc. This circuit has been operating satisfactorily for 11 months and has never required any further attention.

Voltage Measurement

A series of eighty-six 30 megohm metallized, 1 percent 5 watt resistors (Nobleloy) were used as a bleeder in series with a .0038 μa per mm. galvanometer to measure the output high voltage as shown in Fig. (9). A 10^4 ohm resistor was connected in series with the galvanometer and this combination was shunted with a decade resistor box. The high voltage was turned up to approximately the voltage desired, as indicated by a microammeter in series with the galvanometer circuit. Then the decade shunt resistance was increased until the galvanometer read 97 mm. Whenever it was desired to repeat this voltage, the decade would be set to the resistance previously used, and the voltage increased until the galvanometer read 97 mm. The galvanometer circuit was subsequently calibrated with a sensitive potentiometer (Rubicon) with the decade resistance set and the galvanometer reading 97 mm. Thus the voltages were determined to 1 percent accuracy.

Output Voltages

As well as the output points at each stage on the voltage multiplier, there was a potential divider across the top stage of the multiplier, from which focussing voltages could be obtained. A series of fourteen 30 megohm resistors, identical with those used in the bleeder resistor were placed across the "d-c" condenser of the last multiplier stage. Thus when the main high voltage output was altered, the focussing voltage could be kept approximately constant by appropriate adjustment of clip lead connections to the potential divider.

The high voltage bleeder, and the focussing voltage potential divider were placed in a lucite box which was separate from the one containing the voltage multiplier circuit. The resistor box was divided into two sections; one section containing the bleeder resistor, and which was filled with oil, the other which contained the potential divider which was not oil filled. It was found that because the latter section was well isolated from other parts of the circuit, and from ground, there was no corona discharge from it even at the highest voltages used.

High Voltage Supply Performance

The circuit described has been in successful operation for 11 months and has given no trouble. However it must be pointed out that due to the stray capacitance across the two branches of the multiplier circuit, large r-f circulating currents are present. Hence there is power loss in the r-f transformer secondary, the ballast inductance L_b and in the condensers etc. The efficiency of the multiplier circuit is only about 10 percent. The inductance L_b keeps the ripple to less than 0.2 percent but it does not cut

out the power loss due to the circulating currents. The largest part of the stray capacity is introduced by the filament circuit isolating transformers. The oil increases this by a factor of 2.3. However no matter what component spacing is used, oil immersion is necessary for voltages of the magnitude used here; otherwise, there would be corona discharge from the innumerable sharp edges of the tube mounts, condensers, coils, etc.

However the circuit does have certain advantages. The relatively high operating frequency allows the use of small and hence inexpensive components. The input r-f transformer, and the condensers, are much smaller than would have been necessary were the frequency much less than it was. The voltage multiplier was compact; the lucite box measured 37 1/2 inches by 7 inches by 2 1/2 inches.

The maximum voltage obtained from the circuit was 93 kv. At this output voltage the r-f transformer required cooling by a compressed air blast.

Because of the well regulated 600 volt power supply, the output voltage was very stable. After a warm up time of 10 or 15 minutes the output remained steady to within 1 percent. This performance was only true however under no load conditions. When the ion source was on, and hence a beam accelerated down the tube, spurious discharges within the tube caused momentary voltage fluctuations; other factors caused the output to drift slowly. However, in most cases this drift was only about 2 percent per hour and could easily be corrected. As an example of output voltage variation with beam current, it was noted that when a 20 μa beam accelerated through 70 kv was suddenly cut off, the output rose to 75 kv. There was no difference in output voltage whether or not all the apparatus such as accelerator tube, motor generator mount, etc. were attached to the set. This was taken as an indication that there was negligible leakage through these units.

Experimental Attachments

In experiments where gaseous targets are used, isolation of the target from the accelerator presents a problem. In many cases the gas chamber is sealed by means of an organic foil on which is evaporated aluminium (37). The main objection to this method is that the beam is very seriously scattered even in the thinnest windows available. Another objection is that no such window can have a perfectly even thickness across its entire surface, and hence particles penetrating one part of the foil will emerge with a different energy from those penetrating another part. The effective window thickness varies during a run; the aluminium tends to sputter under ion bombardment, the organic backing sometimes does not burn off completely, and a thin deposit of oil from the diffusion pumps becomes carbonized as a layer on the foil. Some experimentation prior to carrying out the present work showed that the foils would not stand up to a current density greater than a few microamperes per square centimeter. These considerations led to using isolating capillaries instead of foils.

It has been shown that the rate at which gas at low pressure passes through a tube is proportional to the cube of the radius, and inversely proportional to the length (43). However the fraction of a well collimated ion beam whose cross-sectional area is greater than that of the tube, passing through a long straight tube is obviously proportional to the square of the radius and independent of the length of the tube. Experimentation showed that in the present apparatus a capillary 0.5 mm. in diameter, 2 cm. long would isolate a gas chamber at 5 mm. Hg from the accelerator so that the accelerator pressure rose no more than 6×10^{-4} Hg; that is, the accelerator still functioned properly.

The present experiment required that the beam enter a chamber in which the pressure could be raised from .001 to about .25 mm. Hg, and after passing through this chamber enter another, the pressure of which could be varied from 10^{-4} to 10^{-2} mm. Hg. Isolating capillaries were designed accordingly.

At the target end of many accelerators of this type there is an electromagnet which both analyses the accelerated beam into its components, and accurately deflects the desired component onto the target. However the distance through which the beam must pass without any focussing is greatly increased by the addition of this magnetic field and the beam tends to defocus due to gas scattering and to electrostatic interaction between the ions. The present apparatus had no such adjustable field incorporated in this region. This meant that the capillaries isolating the experimental chambers from the accelerator had to be adjustable so as to admit the ion beam. Thus all components of the beam entered the target chambers. The various components were subsequently analysed in a fixed magnetic field in the Observation Chamber.

A full scale diagram of the equipment used is shown in Fig. (12).

Bolted to the base of the accelerator was a capillary adjustment assembly. The capillary was a brass tube 4.7 mm. O.D., 1.0 mm. I.D. and 3.8 cm. long. Its lower end was sealed by a system of "O" ring seals as shown, but was held loosely enough that it could be moved about with ease. The capillary was held more or less centrally in a brass housing of 9.5 mm. I.D. so that the capillary could be moved as much as 2.4 mm. in any direction from centre, by eight adjustment screws. The capillary could be adjusted to admit a maximum of beam current to the Ion Exchange Chamber.

Ion Exchange Chamber

After passing through the capillary just described, the beam entered the Ion Exchange Chamber where the gas pressure could be varied from 2×10^{-4} mm. Hg. to .25 mm. Hg. On the front of this chamber was a glass observation window which allowed visual observation of the beam. Through the side of this chamber was a small insulated probe which could be inserted into the path of the beam, and used for assisting in alignment of the first capillary.

Pressure in this chamber could be controlled by two means. For evacuation to the lowest pressures desired, (2×10^{-4} mm. Hg) a tube connected this chamber to a point just above the first capillary, inside the main accelerator. For Ion Exchange Chamber pressures greater than a few microns this pumping line was sealed off, and a gas handling system which was connected into the side of the chamber, used to control the gas pressure. This system comprised a 1 litre ballast, a liquid air trap, a McLeod Gauge, an adjustable hydrogen leak, and a Hyvac pump. The experiment did not call for an accurate determination of the pressure in this chamber and so the gas handling system used was quite adequate.

The hydrogen leak was made by flattening a 1/4 inch diameter silver tube for a distance of three inches over its central portion, and bending it into a semi circle. A threaded screw and nut were used to vary the degree of bending of the tube, and hence the amount of gas that would pass through it. The gas flow could be cut off completely by a stopcock.

Observation Chamber.

The top end of the capillary isolating the Ion Exchange Chamber from the Observation Chamber was held firmly in position as shown. The lower end

could be moved about the centre line by adjustment screws. Thus the axis of the capillary could be set parallel to the beam axis. This capillary was made of soft iron and was much longer than the first one described. This allowed the upper end, where the beam entered, to be well out of the magnetic field, the lower end well inside the field, and the inside of the capillary adequately shielded from the field.

The magnetic field was obtained from two permanent magnets formerly used with magnetrons. Embedded in the brass side walls of the Observation Chamber were soft iron pole pieces of such a shape and size as to accommodate the magnetron magnets and to give a uniform field across a 1/2 inch gap of about 2,4000 gauss. It was necessary that the beam entered the Observation Chamber exactly on centre line of the magnetic field. That is why the top of the second capillary was held firmly to the centre line of the Observation Chamber. However, this meant that the whole chamber had to be adjusted if the axis of the capillary did not coincide with the beam axis. The connection between the housing of the second capillary and the Ion Exchange Chamber allowed for this required movement. In operation, the lower chamber, even with the heavy magnetron magnets attached, was found to be quite easily adjustable by the four screws only two of which are shown in Fig. (12).

Three probes projected into the Observation Chamber through "O" ring seals in the brass base plate. The two outer probes were the beam detectors used for making measurements; the centre probe acted as an aid to aligning the second capillary and also acted as a baffle which allowed only desired beam components near the detectors. Fig. (12) shows details of the detectors, and of the central baffle.

Each detector consisted of a Faraday cup inside a grounded shield. The cup was insulated from and glued to the inside of the shield by formvar varnish. The varnish was subsequently baked. The beam passed between the knife edges of the shield, slit, then past a 2 mm. gap and into the Faraday cup. The knife edges were 1.70 mm. apart. As the whole assembly was situated in a relatively high magnetic field, there was no danger of secondary electrons upsetting the measurements, and so the Faraday cup openings were about 4.5 mm. wide. A small opening in the back of the shield allowed a short lead to connect the cup to a kovar seal in the end of the hollow shaft holding the detector. Shielded cable running through the centre of the shaft connected the kovar seal to a d-c amplifier. The shield and cup assembly could be adjusted to any desired angle by a movable joint as shown.

The centre baffle was used mainly to cut off undesired beam components. The slits shown in the sides formed 2 mm. apertures so that a beam having been collimated by the two 1 mm. diameter capillaries would clear the sides of a slit with 0.5 mm. to spare on either side. The baffle itself was insulated from its shaft by a coat of baked formvar varnish, and was soldered to a kovar seal which sat on the end of the hollow shaft. Thus, when moved up close to the second capillary it could measure the total beam current; this was done whenever the lower capillary required adjustment.

The Observation Chamber pressure was controlled by a separate pumping system. A 1 inch diameter pumping manifold was connected to the rear of the chamber. The metal manifold was connected to a glass system through a 3/4 inch I.D. neoprene tube three inches in length; this flexible connection was necessary so that the Observation Chamber could be moved about. Next to the tubing was a large cold "finger" vapour trap, in which liquid nitrogen was used. Into one side of the glass vapour trap was a hydrogen inlet

connected to a controlled hydrogen leak similar to the one used with the gas handling system of the Ion Exchange Chamber. A five litre per second glass diffusion pump backed by a 0.15 litre per second Welch pump kept the system evacuated. The lowest pressure obtainable in this system was 3×10^{-5} mm. Hg when the Ion Exchange Chamber was evacuated, and 1×10^{-4} mm. Hg when the Exchange Chamber pressure was 5×10^{-2} mm. Hg.

On the front of the Observation Chamber was a glass window for visual observation.

An ionization gauge was attached to the side of the chamber for measurement of pressure.

Operation of the Experimental Chambers

Before the experiment was started, the capillaries of the lower chambers were removed and the beam turned on. Focussing voltages were varied until the beam was properly focussed into a well defined parallel beam. This could be checked visually. In this way the optimum focussing voltages were determined over the range of accelerating voltages used. For this adjustment the room had to be quite dark as the pressure in the chambers was only 2×10^{-4} mm. Hg and hence the beam was not very luminous.

The capillaries were re-inserted and the beam turned on. The small probe in the Ion Exchange Chamber was turned to a position below the first capillary so as to pick up any current coming through. The capillary was then adjusted until a maximum current was recorded by the probe. This current was usually of the order of 15 to 20 microamperes. The probe was then moved out of the beam path. The beam could then be seen to strike a point near the second capillary - a small bluish spot was visible. The centre probe of the Observation Chamber was then moved up close to the bottom

of the second capillary and the chamber adjusted until a maximum current was recorded at this probe.

Under normal conditions these adjustments could be made quite readily; however, if, as happened sometimes, the beam were unsteady, it was difficult to line up the capillaries properly. The centre probe was now moved to the bottom of the Observation Chamber and the detectors moved about until they picked up the desired beam components. The beam, of course, having left the second capillary, was analysed by the magnetic field.

There were many "O" ring seals, carrying movable parts of the apparatus, which could cause leaks and hence contaminate the hydrogen used in the experiment. To check the efficiency of the seals the system was pumped down and sealed off from all three pumps. It was found that the leak rate from all parts of the system was indicated by a pressure rise of 6×10^{-3} mm. Hg per hour into the 10 litre volume of the system. During a run all sections were continuously pumped, hence there was no danger of air affecting the measurements.

Accelerator Performance

The maximum beam current obtained in the accelerator was 42 microamperes. The beam was analysed in the magnetic field and its composition determined. It consisted of protons and of molecular ions of mass two and mass three. The ratios of the components varied from day to day. The proton intensity varied from 12 to 30 percent. An example of beam analysis can be seen in Fig. (14). It was not necessarily undesirable that such a large fraction of the beam was molecular. In the experiment, the molecular ions were useful for the production of protons of energies 1/2 and 1/3 the lowest stable accelerating energies obtainable from the accelerator.

The ions could be focussed to a narrow parallel beam which under most circumstances was quite steady both in magnitude and position. About half of the beam could be directed through the top capillary which was 1 mm. in diameter. As in all accelerators of this type, however, occasional spurious discharges took place between the electrodes. Whenever this happened the focussing fields were upset and the beam either defocussed or moved. These discharges usually lasted for only a second or so, but sometimes lasted for as long as a minute; they were observable in a darkened room and the correspondence between them and the beam defocussing was easily seen. They were accompanied by a drop in accelerating voltage of the order of 2 percent or more. This trouble was kept to a minimum by the occasional cleaning of the top electrode with steel wool.

Measurement of (i^-/i^+) and i^-

Current picked up by the detector cups was carried by shielded cable to a resistor circuit shown in Fig. (13), negative (i^-) and positive (i^+) currents going to the appropriately marked input terminals. We have called this the Ratio Resistance Circuit. Any voltage developed at point A was applied directly to the grid of an FP 54 tube incorporated in a d-c amplifier (38). As can be seen, the voltage developed at A is given by

$$i^+ R_4 - i^- (R_1 + R_2 + R_3)$$

Thus if the settings on R_2 and R_3 were varied until this voltage was zero,

$$\frac{i^-}{i^+} = \frac{R_4}{R_1 + R_2 + R_3}$$

On the other hand, the total negative current could be measured by shorting out R_3 and turning the R_2 contact to the low point of R_2 ; i.e. grounding the positive current.

The switch S was used to ground the d-c amplifier in order to check it for balance.

The amplifier was of the DuBridge Brown type (39). The circuit and galvanometer had a sensitivity of $.45 \times 10^{-3}$ volts per mm. An Ayrton shunt reduced the sensitivity by 0.1, 0.01, and 0.001. For most measurements the galvanometer was "zeroed" in the centre of the scale; this "zeroing" was frequently checked throughout a run and never allowed to drift more than 0.2 mm.

The resistors of the Ratio Measurement Circuit were measured to 1 percent accuracy. R_1 was 102.5×10^6 ohms; R_3 was either a 1 or 4 megohm potentiometer, carefully calibrated; R_2 was a series of 1 or 3 megohm resistors depending on the order of magnitude of the ratio (i^-/i^+). Exact values of the resistances are given in Fig. (13).

The net insulation resistance of the detector cups, shielded cables, and terminals, between the detector cups and the grid of the FP 54 tube was measured and found to be greater than 5×10^{10} ohms. This was quite satisfactory since the grid leak resistor (i.e. $R_1 + R_2$ of Fig. 13) of the FP 54 was never greater than about 1.3×10^8 ohms.

Pressure Measurement

The pressure in the Observation Chamber was measured with an Ionization Gauge (N.R.C. type 710) which had been previously calibrated for hydrogen against an accurate McLeod Gauge. The McLeod Gauge was accurate to better than 1 percent; mercury levels in the gauge were measured with a vernier calliper.

Before a series of cross-section measurements were taken, the Observation Chamber was evacuated to about 4×10^{-5} mm. Hg. Hydrogen was then admitted

through the adjustable leak until the desired pressure was reached. Sometimes the pressure could be set at any desired value and it would remain steady, but at other times it fluctuated so as to make a pressure determination difficult. One had to be certain that the pressure recorded by the gauge was, in fact, the same as the pressure in the Observation Chamber.

It was found that the d-c amplifier in the ion gauge would wander off balance during a run, and also that the calibration voltage changed slightly, even though the unit was connected to a voltage-stabilizer transformer.

With the above considerations in mind it was estimated that the best accuracy obtainable for values of p_o was about $\pm$ 5 percent.

PRELIMINARY EXPERIMENTS

Several observations of a minor nature, but relating to the experiment, are desdribed in what follows.

Beam Analysis

The Ion Exchange Chamber was evacuated to 2×10^{-4} mm. Hg, the Observation Chamber to about 4×10^{-5} mm. Hg, and the beam aceelerated to a desired energy. The positive ion detector was moved from top to bottom of the Observation Chamber in steps of about 1 mm. and the current recorded at each point. The analysis of the positive ion beam is shown in Fig. (14). As well as the three main peaks H^+, H_2^+, and H_3^+, there were three much smaller ones. When the pressure p_i was raised to 5×10^{-2} mm. Hg the two peaks at 6.7 and 6.2 cm. increased in size, while the molecular ion peaks all but disappeared, as can be seen in Fig. (15). As will be explained later (cf "Determination of 'd'"), the energy of a proton was uniquely determined by the position of the detector which the proton entered. Hence it was possible to determine with certainty that the peaks at 6.7 and 6.2 cm. were due to protons from the dissociation of H_2^+ and H_3^+ respectively, and that this dissociation took place in the Ion Exchange Chamber. Residual gas in the Ion Exchange Chamber and in the base of the accelerator accounted for the presence of "dissociation protons" at low values of p_i. The origin of the peak at 8 cm. was likewise established, viz. H_2^+ from the dissociation of H_3^+.

The analysis of the negative components of the beam emerging from the Ion Exchange Chamber was similarly determined. When the pressure p_i was low, there were three ion peaks which corresponded in psoition to the three proton peaks of the positive beam analysis. When p_i was increased to 5×10^{-2} mm. Hg the three negative peaks greatly increased in size. The negative peaks for

for both high and low p_i are shown in Fig. (16). Thus it was established that the negative ions were of mass one only, and that no negative molecular ions were formed.

Equilibrium Ratio

With both experimental chambers evacuated, the detectors were placed so as to collect the protons and negative ions whose energy corresponded to that of the proton component of the beam incident on the Ion Exchange Chamber. The galvanometer of the d-c amplifier was then brought to zero by adjusting the Ratio Resistances as previously described; the resistances R_3 and R_4 were recorded. The negative current was then determined by grounding the positive current and reading the galvanometer deflection. The pressure in the Ion Exchange Chamber was then increased in steps and the ratio (i^-/i^+) and the galvanometer deflection for i^- recorded at each step. The Observation Chamber pressure, p_o, was obtained from the ionization gauge and recorded. Fig. (17) shows how the ratio reached an equilibrium value $(i^-/i^+)_e$.

It is to be pointed out that since

$$\left(\frac{i^-}{i^+}\right) \cdot \left(\frac{i^-}{i^+}\right)_e e^{-(\sigma_2 - \sigma_1) \kappa p_o d}$$

(cf Theory) and since p_o rose slightly as p_i was increased, then the values of (i^-/i^+) at high values of p_i were not exactly equal to $(i^-/i^+)_e$. The pressure p_o as read from the ionization gauge provided the information necessary to correct the values of (i^-/i^+) at the higher pressures p_o to give $(i^-/i^+)_e$. This correction was made before plotting the values shown in Fig. (17). A similar correction was applied to i^-.

The value of the equilibrium ratio, $(H^-/H^+)_e$, depended only on the energy of the atomic ions involved and did not depend on the source of the ions (i.e. whether they arose from the dissociation of molecular ions or came from the original proton beam). This was shown by the following test. The ratio $(H^-/H^+)_e$ was measured for a 12 kv. proton beam, for the beam of

protons arising from the dissociation of an H_2^+ beam which had been accelerated to 24 kv, and for the beam of protons from an H_3^+ beam accelerated to 36 kv. In all cases the ratio $(H^-/H^+)_e$ was the same within the limits of error of measurement.

Gas Scattering

The variations of i^- and i^+ with p_i are shown in Figs (18) and (19). Whereas their ratio reached an equilibrium value, the negative and positive currents themselves did not reach equilibrium. This has been attributed to gas scattering in the Ion Exchange Chamber. In order to investigate this, the gas was considered as a foil and the formula for multiple scattering was applied (40). This formula explained the observed scattering. Now the solid angles subtended by the detectors (in the Observation Chamber) at points within the Ion Exchange Chamber were much smaller than the solid angles subtended at points in the Observation Chamber. That is, small angle scattering in the Ion Exchange Chamber would affect the number of particles reaching the detectors to a much greater extent than would the same degree of scattering in the Observation Chamber. By applying the scattering formula to interactions in the Observation Chamber it was established that gas scattering in this region was negligible. A further point of note is that the pressure in the Ion Exchange Chamber was usually 5×10^{-2} mm. Hg, whereas the maximum pressure in the Observation Chamber was only 1.2×10^{-2} mm. Hg.

Another check on scattering was made by moving a detector across a beam in the Observation Chamber when the pressure p_o was at its maximum value, and comparing the width in this case with the width in the case where the pressure p_o was low. There was no observable difference in beam width. This was consistent with the findings of Ribe (30).

Multiple Charge Exchange

Fig. (20) shows the relative positions of the positive and negative

components of the beam in the Observation Chamber after the beam has reached equilibrium in the Ion Exchange Chamber. The subscripts 1, 1/2, and 1/3 refer to atomic ions arising from the original proton component, the mass two molecular component, and the mass three molecular component, respectively, in the accelerator beam which was incident on the Ion Exchange Chamber. It was stated that when the Observation Chamber pressure p_o was raised, the positive ions would capture electrons from the gas atoms and would leave their curved paths tangentially; the negative ions, of course, would lose an electron and similarly leave their paths. In the diagram the detectors are placed so as to receive particles which have energies corresponding to the full accelerating potential of the accelerator. At low pressures p_o, the beams of $H_{1/2}$ and $H_{1/3}$ did not interfere with the measurements on H_1. However as p_o was raised, ions of $H_{1/2}$ and $H_{1/3}$ were neutralized and left the curved paths shown. Some of the resultant neutral atoms were re-ionized and a fraction of those then entered the detectors; in the case of i^+, the current to the detector was erroneously high. That is, as the pressure p_o increased, the current i^+ did not drop off as rapidly as it would have had there been no interference; calculation of α' under these circumstances gave a value considerably less than would have been obtained had there been no such interference.

The purpose of the central baffle was to allow only the desired negative and positive ions to reach the detectors. The other beams were effectively blocked and could not contribute appreciable error to the measurements. The position of the baffle has been dotted in on the diagram.

This process of multiple charge exchange could also contribute to the error of measurement by taking place within the beam that was being detected due to the fact that the detector aperture had a finite width. Consider a

proton in the curved path and fairly close to the detector. If it captures an electron, leaves its curved path, and becomes ionized again before it has gone too far, it could enter the detector and be recorded. This process has been studied rather carefully by Kanner (41) who showed that in his apparatus the effect was negligible so long as the product $n\sigma_{\ell'} < 0.2$. The geometry of the present apparatus was similar enough to that of Kanner's to allow the same criterion to be used. A calculation of the maximum value of $\sigma_{\ell'}$ was obtained from the work of Bartels (24). The maximum pressure used in the Observation Chamber was 1.2×10^{-3} mm. Hg. Thus the maximum value of $n\sigma_{\ell'}$ in the present experiment was

$$n\sigma_{\ell'} = 7.7 \times 10^{14} \times 9 \times 10^{-17}$$
$$= .07 .$$

It is safe then to assume no error arises from multiple charge exchange in the proton beam. A consideration of a similar process taking place in the negative ion beam again shows that errors arising from multiple exchanges in this beam would not be appreciable.

Magnetic Shielding

If there were an appreciable magnetic field either in the Ion Exchange Chamber, or inside the lower capillary, the beam would be partially analysed in these regions and some of the ions would strike the side walls of the capillary before they entered the Observation Chamber. A check for this was made by altering the position of the Observation Chamber and also by adjusting the alignment of the lower capillary. Had there been stray fields, such adjustments would have changed the ratio (i^-/i^+) at the detectors, increasing it as the capillary was moved in the direction of the negative ion probe, decreasing it as it was moved toward the positive probe. When the soft iron capillary was used no such effect was observed. When a non magnetic

material (brass) was used for the capillary, this effect was very pronounced. In fact the ratio could be varied by a factor of three by a slight adjustment of the lower capillary.

Formation of H^-

In order to make certain that the negative ions were formed by the interaction of protons with gas molecules, and not by their interaction with the walls of the capillary through which they passed, the capillaries were removed and the ratio (H^-/H^+) measured. It was of course small ($\sim$ .05 percent at 40 kv), but still there was enough residual gas to produce a few negative ions. The ratio was measured again with the capillaries in place and was found to be the same.

As a further check, the hydrogen in the Ion Exchange Chamber was replaced with air. In this case the equilibrium ratio of (i^-/i^+) was much lower than it was for hydrogen. At 50.5 kv the ratio with air was 0.52 percent while with hydrogen it was 1.5 percent.

In any event, it is difficult to see how the beam in the Observation Chamber could have been as well collimated as it was if an appreciable number of particles in the beam were interacting with the metal walls of the capillary.

It has already been mentioned that movement of the capillaries did not alter the ratio (i^-/i^+) in any way. Had the metal capillaries been responsible for the production of the H^- ions, the results of such an adjustment would have been different.

Energy Loss in the Gas

An attempt was made to determine the extent of the energy loss of the

particles passing through the Ion Exchange Chamber when the pressure p_i was 60×10^{-3} mm. Hg. This chamber was evacuated (as was the Observation Chamber throughout this test) and a detector set to pick up a maximum of the proton beam. The pressure p_i was then raised to 60×10^{-3} mm. Hg and the detector adjusted in order to determine if there had been a change in the position of the peak. A 2 percent energy change could have been detected. However, no shift in the peak was observed even at the lowest energy, 4.2 kv. In the low energy case, the $H^+_{1/3}$ beam was used; thus there was no detectable energy loss by the molecular beams either.

Determination of "d" (cf. Fig. (2))

Because the magnetic field was fixed the energy of an atomic ion entering a detector was uniquely determined by the position of the detector. From the geometry of the Observation Chamber there was established a relation between the positions of the detectors and the path distances "d" of the ions in this chamber. Thus, by setting a detector to collect an atomic beam in the Observation Chamber, and by observing the position of the detector, the path distance "d" for the ions collected could be determined.

There was some uncertainty as to the lengths of these paths. Between the detector shield and the collector cup was a 2 mm. gap. If an ion lost its charge in this region it was a matter of doubt just from where the neutralizing charge ultimately came. If the event took place near the shield, the effective source of that charge would probably be the shield; if it were near the Faraday cup, the incident ion would probably contribute to the current collected by the cup.

Smaller uncertainties arose due to end effects at the entrance capillary and to errors in measurement of the detector positions.

From these considerations the uncertainty of measurement of "d" was estimated to be $\pm$ 2 mm.

EXPERIMENTAL PROCEDURE

Both chambers were evacuated and the detectors adjusted to pick up the negative and positive beam components desired. Where the output of the high voltage supply could be adjusted to the desired energy value, components corresponding to the original proton beam were used. For energies lower than the minimum accelerating voltage, the components arising from the molecular beams were used. Thus although the minimum voltage was 12.6 kv, the mass three molecular component provided, after the molecular ions had been dissociated by collisions with gas in the Ion Exchange Chamber, positive, negative, and of course, neutral particles of 4.2 kv energy.

The Ion Exchange Chamber pressure p_i was increased and the ratio (i^-/i^+) noted until a further increase in pressure produced no corresponding increase in ratio. At all energies used, equilibrium was attained before the pressure reached 5×10^{-2} mm. Hg, so throughout the experiment p_i was set at between 5×10^{-2} mm. and 6×10^{-2} mm. Hg.

The ratio (i^-/i^+) and the deflection due to i^- were recorded. The centre baffle was then adjusted so as to cut off the undesired beams yet pass the desired two. The pressure in the Observation Chamber, p_o, was increased in steps and readings of (i^-/i^+) and i^- taken. As the maximum hydrogen pressure that the ionization gauge would read was about 1.2×10^{-3} mm. Hg, this was the highest pressure used. The pressure p_o was then decreased in steps and readings taken each time until low p_o was reached again. This procedure was repeated two or three times. The detector positions were measured. A typical example of one of six runs made at 25.6 kv is shown in Fig. (21).

The (i^-/i^+) and i^- values were plotted on semi-log paper against p_o in units of 10^{-3} mm. Hg. The ion path distance, "d", was obtained from the positions of the detectors; the value of k (cf. p.11) was obtained from a

knowledge of the temperature as read from a thermometer.

The electron loss cross-section for negative ions was calculated by dividing the average of the slopes of the i^- curves by the product kd.

The electron capture cross-section for protons was calculated by dividing the average of the differences between the slopes of the i^- curves and the (i^-/i^+) curves by kd.

The ratio $(H^-/H^+)_e$ was obtained by averaging the ordinate intercepts of the (i^-/i^+) curves.

At the lower energies the slopes of the negative ion curves were sufficiently greater than those of the ratio curves that the curves could be drawn in by eye, slopes calculated, differences taken, and the capture cross-section for protons evaluated with very little error in comparison to the uncertainties due to path distance and pressure. However at 50.5, 60.4, and 70.3 kv, the slopes of the two curves were so close that least squares determinations of these curves were made.

The values of $(H^-/H^+)_e$, σ_l , and σ_c, have been listed in Table I. The variation of these quantities with energy has been plotted in Figs. (22), (23), (1).

TABLE I

E kv	s_-	s_+	$s_+ - s_-$	d cm.	T°A	$k \times 10^{-13}$	$\sigma_e \times 10^{16}$ cm^2	$\sigma_{e'} \times 10^{16}$ cm^2	$(H^-/H^+)_\infty$%
4.2	.194	.067	.127	4.88	302	6.40	6.3 ± .4	4.2 ± .3	13.2 ± .5
6.9	.211	.067	..144	5.25	302	6.40	6.3 ± .4	4.3 ± .3	20.8 ± .8
8.5	.233	.077	.156	5.45	302	6.40	6.7 ± .4	4.5 ± .3	22.2 ± 1.3
10.3	.228	.079	.149	5.72	302	6.40	6.3 ± .4	4.1 ± .3	20.9 ± .5
15.2	.229	.083	.146	6.15	302	6.40	5.8 ± .3	3.7 ± .2	14.4 ± .4
20.6	.197	.087	.110	6.60	299	6.46	4.6 ± .3	2.6 ± .3	9.7 ± .6
25.6	.185	.086	.099	6.80	301	6.42	4.3 ± .3	2.3 ± .2	6.5 ± .3
30.4	.177	.095	.082	6.90	297	6.50	4.0 ± .2	1.8 ± .2	5.0 ± .1
35.0	.164	.095	.069	7.05	297	6.50	3.6 ± .2	1.5 ± .1	3.8 ± .2
40.1	.161	.102	.059	7.32	297	6.50	3.4 ± .2	1.24 ± .10	2.8 ± .1
50.5	.149	.103	.046	7.66	297	6.50	3.0 ± .2	0.92 ± .09	1.48 ± .05
60.4	.139	.109	.030	8.08	297	6.50	2.7 ± .2	0.56 ± .04	0.89 ± .03
70.3	.135	.119	.016	8.30	297	6.50	2.5 ± .2	0.30 ± .06	0.52 ± .02

Where, s_- is the average of the slopes of the curves of ln H^- vs. p_o.
s is the average of the slopes of the curves of ln (H^-/H^+) vs. p_o.
E is the energy of the incident protons.
d is the ion path distance in the Observation Chamber

$$\sigma_e = \frac{s_-}{kd}$$

$$\sigma_{e'} = \frac{s_- - s_+}{kd}$$

ERRORS

A sample calculation of σ_i and σ_e, including a calculation of probable error has been given in Appendix II. The error calculation included ± 5% for uncertainty in p_o, ± 0.2 cm. for uncertainty in "d", and the "probable error of the mean" of the six runs. As well as the calculable error there may have been other errors which were difficult to evaluate. However the cumulative error in σ_i is probably not greater than 10 percent. Below 40 kv the error in σ_e is probably not greater than 10 to 15 percent, but above this energy the error could be between 15 and 30 percent.

Each resistance of the Ratio Resistance Circuit was measured to ± 1 percent; however, indeterminacy of calibration and reading of the potentiometer would contribute to error in the measurement of $(H^-/H^+)_e$. Fluctuations in the values of (i^-/i^+) added considerably to the uncertainty in $(H^-/H^+)_e$. The uncertainties listed in Table I include those due to the fluctuations. The cumulative error of measurement of $(H^-/H^+)_e$ should not be greater than ± 7 percent.

DISCUSSION OF RESULTS

The Equilibrium Ratio $(H^-/H^+)_e$

Fig. (22) shows that the ratio $(H^-/H^+)_e$ increases rapidly as the proton energy decreases, and reaches a maximum of 22.2 percent at 8.5 kv. This rather high value would indicate that the results of experiments carried out to obtain values for $\sigma_{c'}$ and $\frac{\sigma_{\ell'}}{\sigma_{c'}}$ might have been in error where the presence of H^- was not considered. This will be discussed presently.

The Electron Loss Cross-Section for Negative Hydrogen Ions

A comparison of Fig. (23) with Fig. (1) shows that σ_ℓ varies much less rapidly with energy than does $\sigma_{c'}$. It is interesting to note that Montague (29) found that the electron loss cross-section for netural hydrogen atoms ($\sigma_{\ell'}$) also varied slowly with energy.

The Electron Capture Cross-Section for Neutral Hydrogen Atoms

It was shown in the section on Theory that the relation between the various cross-sections and $(H^-/H^+)_e$ was,

$$\left(\frac{H^-}{H^+}\right)_e = \frac{\sigma_{c'}}{\sigma_{\ell'}} \frac{\sigma_c}{\sigma_\ell}$$

There is fair consistency between the values of $\frac{\sigma_{\ell'}}{\sigma_{c'}}$ as found by Montague and Ribe (30), and those calculated from the observations of Bartels (24) where the two sets of results overlap between 45 kv and 60 kv. Due to the fact that the presence of H^- in the experiment of Bartels was not considered, $\frac{\sigma_{\ell'}}{\sigma_{c'}}$ cannot be calculated directly from the values he gave for $(H^+/H^o)_e$, since it is apparent that what he actually measured was $\left(\frac{H^+ + H^-}{H^o}\right)_e$. Thus, referring to his values as w,

$$\left(\frac{H^+ + H^-}{H^o}\right)_e = \omega$$

Then,

$$\left(\frac{H^-}{H^o}\right)_e = \omega - \left(\frac{H^+}{H^o}\right)_e$$

Putting

$$\left(\frac{H^o}{H^+}\right)_e = r,$$

then $H_e^- = rH_e^+$ and so

$$r\left(\frac{H^+}{H^o}\right)_e = \left(\frac{H^-}{H^o}\right)_e = \omega - \left(\frac{H^+}{H^o}\right)_e$$

and thus

$$\left(\frac{H^+}{H^o}\right)_e = \frac{\omega}{1+r}$$

gives the corrected value of $\left(\frac{H^+}{H^o}\right)_e$.

But it was shown that

$$\left(\frac{H'}{H^o}\right)_e = \frac{\sigma_{e'}}{\sigma_{c'}}$$

Thus, the corrected values of Bartels and the values of $\frac{\sigma_{e'}}{\sigma_{c'}}$ obtained by Montague and Ribe, give a set of values for $\frac{\sigma_{e'}}{\sigma_{c'}}$ over the whole range of the present experiment. With these values and the known values for $(H^-/H^+)_e$ and σ_l, the calculation for σ_c can be made from the relation

$$\sigma_c = \left(\frac{\sigma_{e'}}{\sigma_{c'}}\right)\left(\frac{H^-}{H^+}\right)_e \sigma_l$$

This has been done, and a curve of σ_c against energy is shown in Fig. (24). It is difficult to estimate the accuracy of these values, but over most of the energy range shown it is felt that the uncertainty does not exceed 20 percent.

The Electron Capture Cross-Section for Protons

With a view possibly to modifying the values of α_1 (cf. Fig. (1)) found by Bartels by consideration of the ions H^-, the Wien formula used by him was investigated. Due to the complexity of the exact expressions for H^+, H^o, and H^- a corrected Wien formula is not possible. However, numerical calculation shows that the Wien formula is correct to about $\pm$ 1 percent at 7 kv (where H^- production is a maximum) when the proper values of (H^+/H^o) and

$(H^+/H^0)_e$ are used. Indeed, if $(\frac{H^+ + H^-}{H^0})$ and $(\frac{H^+ + H^-}{H^0})_e$ are used instead, as was done by Bartels, the error involved is only about 3 percent. Hence there appears to be no explanation of the high peak of Bartels' on the basis of negative hydrogen ions. Since, however, H^- ions will affect the calculation of $\frac{\sigma_{ii'}}{\sigma_{ii'}}$ which is numerically equal to $(H^+/H^0)_e$, and since the values of are not affected, then to find $\sigma_{ii'}$ from Bartels' work one must make a correction.

Due to the method used, the observations of Keene (21) (cf. Fig. (1)) were not appreciably affected by H^-. He stated that the cumulative error in his values did not exceed $\pm$ 10 percent. Thus within the limits of error the results of Keene, and those of the present work are in fair agreement. Also within the limits of accuracy of the two experiments, the present values of those of Ribe agree. This is especially true at the low energy end of the latter's curve where the accuracy of the present work is much better than it is at the higher energies (cf. Theory).

Neither the results of Meyer, nor those of Smith were appreciably affected by negative hydrogen ions.

The peak at about 7 kv in the $\sigma_{ii'}$ curve has no theoretical explanation as yet.

Included in Fig. (1) is a theoretical curve for the capture cross-section due to J.D. Jackson and H. Schiff (unpublished). These theoretical results were obtained by using the Born approximation (believed to be valid in this particular problem even for velocities such that $\frac{h\nu}{e^2}$ is of order unity), and includes captures into all excited states. Earlier theoretical work was done by Brinkman and Kramers (44) who also used the Born approximation but neglected part of the interaction. Their formula gave results approximately four times larger than recent experiments in the energy range considered.

A theoretical calculation of the electron capture cross-section for neutral hydrogen atoms is much more difficult than the corresponding calculation for protons. However Jackson has recently completed a calculation of the ratio $\frac{\sigma_s}{\sigma_c}$, for proton energies where $v \gg v_o$ (i.e. where the velocity of the proton is much greater than the orbital velocity of an electron in the ground state of the hydrogen atom). The limiting value of this ratio for high energy was 0.16 (private communication). The experimental results of the present experiment show that $\frac{\sigma_s}{\sigma_c}$ increases from about .04 at 10 kv, to about .08 at 70 kv. One would not expect the ratio to have reached its limiting value at such relatively low energies and so the theoretical and experimental results are not inconsistent with each other.

CONCLUSION

A proton accelerator of the Cockcroft-Walton type was designed and built. Accelerating potentials were obtained from a high voltage supply of novel character in that radio-frequency power was used to operate a seven stage voltage-multiplier circuit. The fourteen diode rectifiers of the multiplier circuit obtained filament power from a series of r-f isolating transformers. This method of supplying heater voltages had not been used previously. Apparatus was designed for ion analysis after charge exchange had taken place.

A beam of protons was directed through hydrogen gas and the formation of negative hydrogen ions in the beam was investigated. The proton energies ranged from 4 to 70 kv. When the beam had traversed sufficient gas, the ratio of negative ions to protons reached an equilibrium value. This equilibrium ratio varied from a maximum of 22.2 percent at 8.5 kv, to 0.52 percent at 70.3 kv.

The electron loss cross-section for a negative hydrogen ion was measured over the same energy range; the cross-section decreased from about 6.7×10^{-16} cm.^{2} at 8.5 kv to 2.5×10^{-16} cm.^{2} at 70.3 kv.

The electron capture cross-section for a proton was measured at the same time and showed fair agreement with values determined in other recent investigations both theoretical and experimental. The energy range over which these values were obtained had not previously been covered by any one investigator.

The results of the present work, combined with those of previous experiments with proton beams, have allowed the calculation of the electron capture cross-section for a neutral hydrogen atom with energies between 4 and 70 kv. This cross-section varied from about 19×10^{-18} cm.^{2} at 10 kv, to 2.5×10^{-18} cm.^{2} at 70 kv.

BIBLIOGRAPHY

(1) O. Tuxen, Z. Physik, 103, 463, (1936).

(2) Hylleraas, ibid. 60, 624, (1930)

(3) Wildt, Ap. J. 89, 295, (1939; 93, 47, (1941)

(4) Deutsch, Rev. Mod. Phys., 20, 388, (1948)

(5) Jen, Phys. Rev., 43, 540 (1933)

(6) Glocker, Phys. Rev., 46, 111, (1934)

(7) Massey and Smith, Proc. Roy. Soc., A155, 472, (1936)

(8) Williams, Phys. Rev. 62, 538, (1942)

(9) Henrich, Phys. Rev., 62, 545, (1942)

(10) Bates, Proc. Roy. Irish Acad., 51A, 151, (1947)

(11) Conwell, Phys. Rev., 74, 277, (1948)

(12) Ionescue, C.R. Acad. Sci., 226, 1005, (1948)

(13) Hylleraas, Ap. J., 111, 209, (1950), 113, 704, (1951)

(14) Arnot and Milligan, Proc. Roy. Soc., A156, 538, (1936).

(15) Arnot and Beckett, ibid. A158, 137, (1937)

(16) Sloane and Watt, ibid. A61, 217, (1948)

(17) Lofgren, Rev. Sci. Inst., 22, 321, (1951)

(18) Hasted, Proc. Roy. Soc., A212, 235, (1952)

(19) Chandrasekhar, Ap. J. 102, 223, (1945)

(20) Massey, "Negative Ions", Cambridge 1938
"Negative Ions", (second edition) Cambridge, 1950.

(21) Keene, Phil. Mag., 40, 369, (1949)

(22) Massey and Burhop, "Electronic and Ionic Impact Phenomena", Oxford, 1952

(23) Goldman, Ann. der Physik, 10, 460, (1931)

(24) Bartels, ibid. 6, 957 (1930)

(25) Wien, Sitz. d. Kgl. Preuz. Acad. d. Wiss. 1911

(26) Rudnick, Phys. Rev. 38, 1342, (1931)

Batho, ibid. 42, 753, (1932)

Meyer, Ann. der Physik 37, 69, (1940)

(27) Keene, Phil. Mag., 40, 369, (1949)

(28) Kallman and Rosen, Z. Physik, 64, 806, (1930)

Rostagni, Nuovo Cimento, 12, 134, (1935)

Wolf, Ann. der Physik 30, 313, (1937)

Sherwin, Phys. Rev., 57, 814, (1940)

Simmons et al, J. Chem. Phys., 11, 316, (1943)

Hasted, Proc. Roy. Soc., A205, 421, (1951)

(29) Montague, Phys. Rev., 81, 1026, (1951)

(30) Ribe, ibid. 83, 1217, (1951)

(31) Bailey and Ward, Can. J. Res. 26, 69, (1948)

(32) Cockcroft and Walton, Proc. Roy. Soc. 136, 619, (1932)

(33) Lamar et al., J. App. Phys. 12, 132, (1941)

(34) Lorrain, Rev. Sci. Inst., 20, 216, (1949)

(35) Mathers, "Radio-Freq. High Voltage Power Supplies", Nat. Res. Coun. of Canada, 1948

(36) Siezen and Kerkhof, Proc. I.R.E., 36, 401, (1948)

(37) Hall, Phys. Rev., 79, 504, (1950)

(38) Eadie, "Stopping Power for Secondary Electrons of Co^{60} in Light Elements" Radiation Lab., McGill University, April, 1949

(39) DuBridge and Brown, Rev. Sci. Inst., 4, 532, (1933)

(40) "Nuclear Physics" (Fermi), Univ. of Chicago Press, 1950, pp. 36,37.

(41) Kanner, Phys. Rev., 84, 1211, (1951).

(42) Smith, Proc. Camb. Phil. Soc., 30, 514, (1934)

(43) Strong, "Proc. in Exptl. Physics", Prentice Hall Inc., 1945, pp. 99

(44) Brinkman and Kramers, K. Wet. Amst., 33, 973, (1930).

APPENDIX I

The solutions from the equations on page 9 are,

$$\frac{H^-}{I} = \frac{b(d-c)}{(ad-bc)} + Ae^{m_1 n x} + Be^{m_2 n x}$$

$$\frac{H^+}{I} = \frac{c(a-b)}{(ad-bc)} + \left(\frac{m_1+a}{b}\right)Ae^{m_1 n x} + Be^{m_2 n x}$$

where

$$a = \sigma_{\ell'} + \sigma_{c'}$$
$$b = \sigma_{\ell'}$$
$$c = \sigma_c$$
$$d = \sigma_\ell + \sigma_c$$

and

$$A = \frac{a+b}{(ad-bc)}\left(d - \frac{d+\frac{bc}{m_1+a}}{1+\frac{m_2+a}{m_1+a}}\right)$$

$$B = \frac{1}{1-\frac{m_2+a}{m_1+a}}\left(\frac{a-b}{ad-bc}\right)\left(d+\frac{bc}{m_1+a}\right)$$

and

$$m_1 = -\left(\frac{a+d}{2}\right) + \sqrt{\left(\frac{a-d}{2}\right)^2 + bc}$$

$$m_2 = -\left(\frac{a+d}{2}\right) - \sqrt{\left(\frac{a-d}{2}\right)^2 + bc}$$

However, to a fair degree of accuracy, the approximate relations

$$\frac{H^-}{I} \doteq \frac{\sigma_c}{\sigma_\ell}\cdot\frac{\sigma_{c'}}{\sigma_{\ell'}+\sigma_{c'}}\left[1 - \frac{2\sigma_\ell - \sigma_{\ell'} - \sigma_{c'}}{\sigma_\ell - \sigma_{\ell'} - \sigma_{c'}}e^{-(\sigma_\ell+\sigma_c)nx} + \frac{\sigma_\ell}{\sigma_\ell - \sigma_{\ell'} - \sigma_{c'}}e^{-(\sigma_{\ell'}+\sigma_{c'})nx}\right]$$

$$\frac{H^+}{I} \doteq \frac{\sigma_{\ell'}}{\sigma_{\ell'}+\sigma_{c'}}\left[1 + \frac{\sigma_{c'}}{\sigma_{\ell'}}e^{-(\sigma_{\ell'}+\sigma_{c'})nx}\right]$$

hold.

The approximate solution for H^+ is what would be obtained were equations (1) and (3) solved, neglecting the formation of H^-. Numerical substitution using experimentally determined values for the cross-sections shows that these approximations are correct to within 5% for the whole energy range 4 to 70 kv; the accuracy is least at 7 kv. but improved for lower or higher energies.

APPENDIX II

Calculation of σ_i and α' at 25.6 kv.

s_-	$\Delta s_- \times 10^3$	$(\Delta s_- \times 10^3)^2$	s_+	$s_- - s_+$	$(s_- - s_+) \times 10^3$	$[(s_- - s_+) \times 10^3]^2$
.188	3	9	.0905	.097	2	4
.184	1	1	.0903	.094	5	25
.180*	5	25	.0855*	.094	5	25
.189	4	16	.0903	.099	0	0
.184	1	1	.0813	.103	4	16
.187	2	4	.0783	.109	10	100
6)1.112		56		6) .596		170
.185				.099		

* Shown in Fig. (21) are the curves from which these values were taken.

$T = 28^{\circ}C.$

$d = 6.8 \pm .2$ cm. ($\pm$ 2.9%)

$$k = \frac{1.93}{T} \times 10^{16} = \frac{1.93}{301} \times 10^{16} = 6.41 \times 10^{13}$$

$$\sigma_c' = \frac{s_- - s_+}{kd} = \frac{.099}{6.41 \times 10^{13} \times 6.8} = 2.28 \times 10^{-16} \text{ cm.}^2$$

$$\sigma_i = \frac{s_-}{kd} = \frac{.185}{6.41 \times 10^{13} \times 6.8} = 4.25 \times 10^{-16} \text{ cm.}^2$$

The "probable error of the mean" of s_- $= .675\sqrt{\frac{\Sigma(\Delta s)^2}{n(n-1)}}$

$$= .675\sqrt{\frac{56 \times 10^{-16}}{6 \times 5}}$$

$$= .009 \text{ (0.5\% of } s_-)$$

Similarly the "probable error of the mean" os $s_+ = .675\sqrt{\frac{170 \times 10^{-6}}{6 \times 5}}$

$$= .0016 \text{ (1.6\% of } s_+)$$

The uncertainty of $p_o = 5\%$

Thus, the total probable percent error in $\sigma_i = \sqrt{(0.5)^2 + (2.9)^2 + (5)^2}$

$$= 5.8\%$$

A similar calculation gives the probable percent error in $\sigma_{c'}$ as 6 percent. Thus,

$$\sigma_{\ell} = (4.25 \pm .25) \times 10^{-16} \text{ cm.}^2$$

$$\sigma_{c'} = (2.28 \pm .14) \times 10^{-16} \text{ cm.}^2$$

ELECTRON CAPTURE CROSS-SECTION FOR PROTONS ($\sigma_{c'}$)

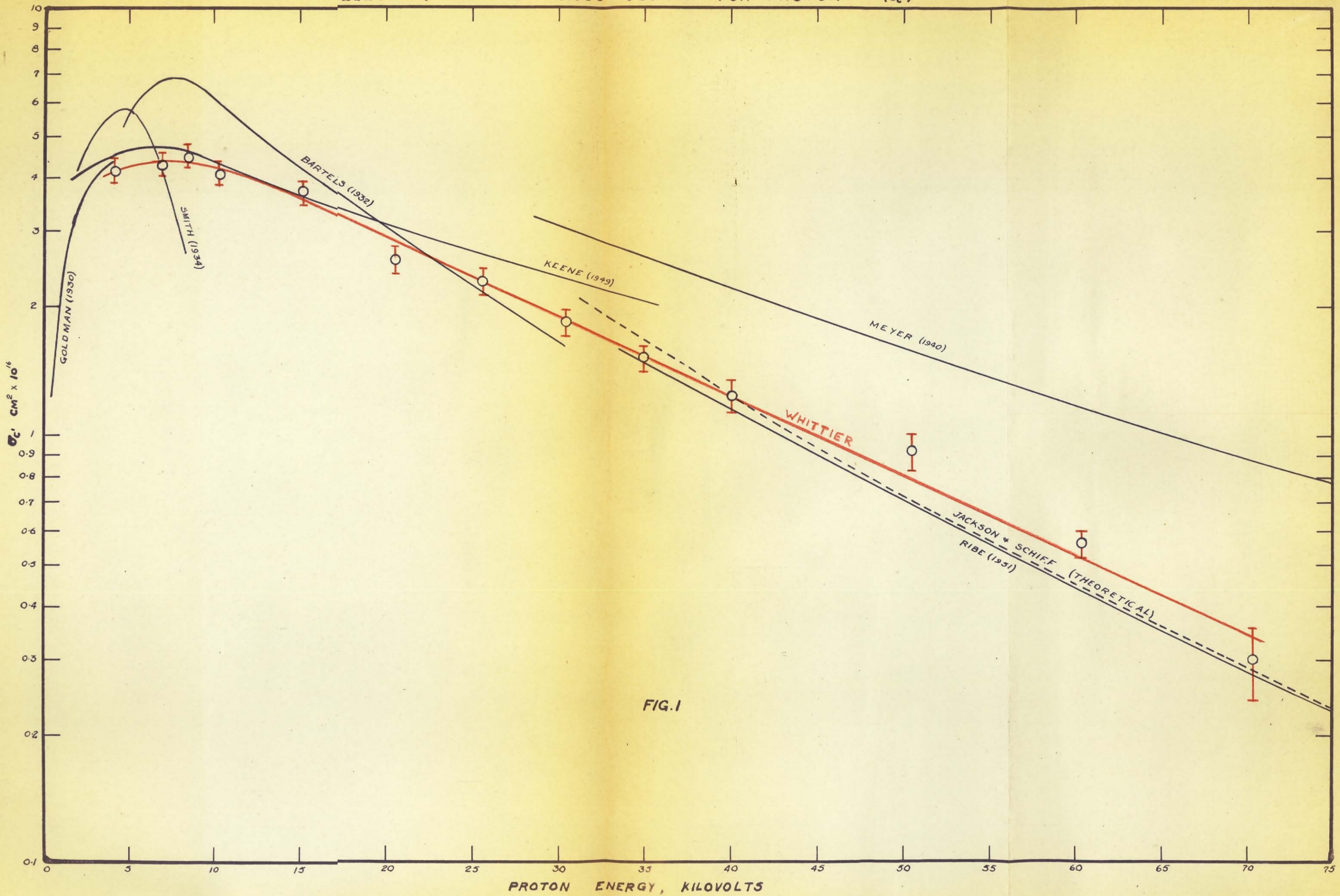

FIG. 1

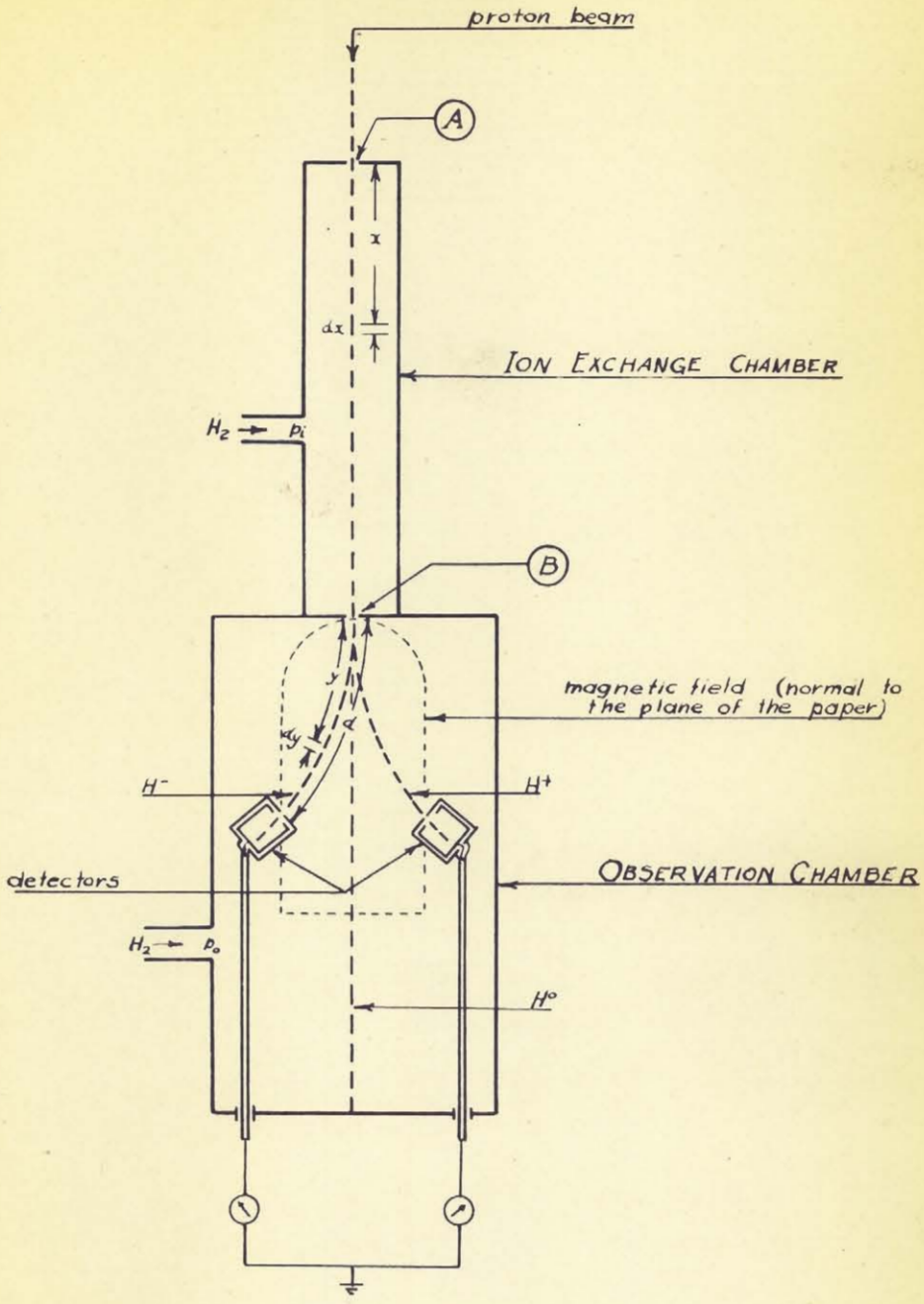
proton beam
A
x
dx
ION EXCHANGE CHAMBER
H_2 → p_i
B
magnetic field (normal to the plane of the paper)
y
α
H^-
H^+
detectors
OBSERVATION CHAMBER
H_2 → p_o
H^o

FIG. 2

ION SOURCE

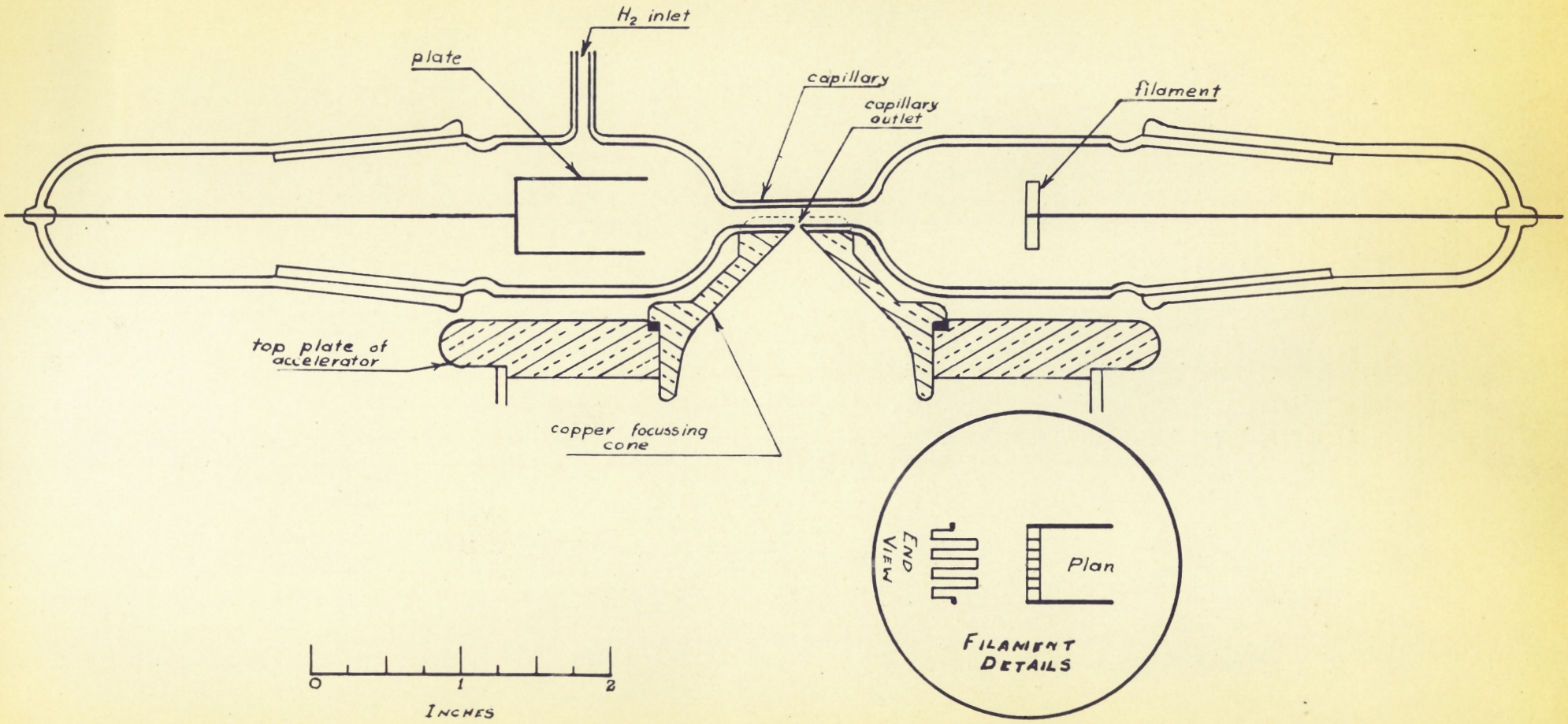

FIG. 3

ION SOURCE WIRING DIAGRAM

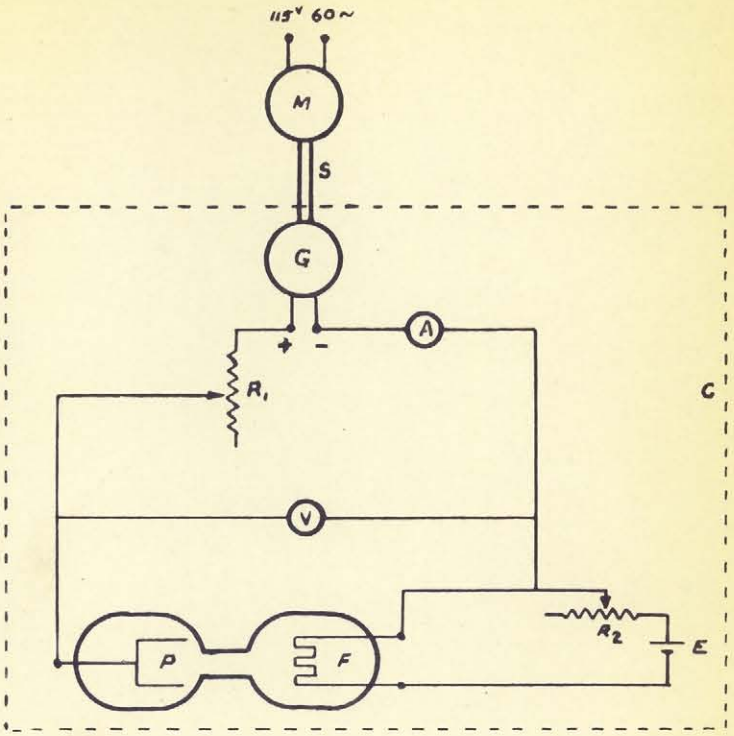

M - 1/4 h.p. a.c. motor
G - 110V d.c. generator
A - 0-1 amp. ammeter
V - 0-250 volt. voltmeter
R_1 - Current limiting potentiometer
R_2 - Filament current potentiometer
F - Filament of Ion Source
P - Plate of Ion Source
E - 4 volt battery
S - Bakelite insulating shaft
C - All equipment within the broken line at high potential

FIG. 4.

ACCELERATOR TUBE

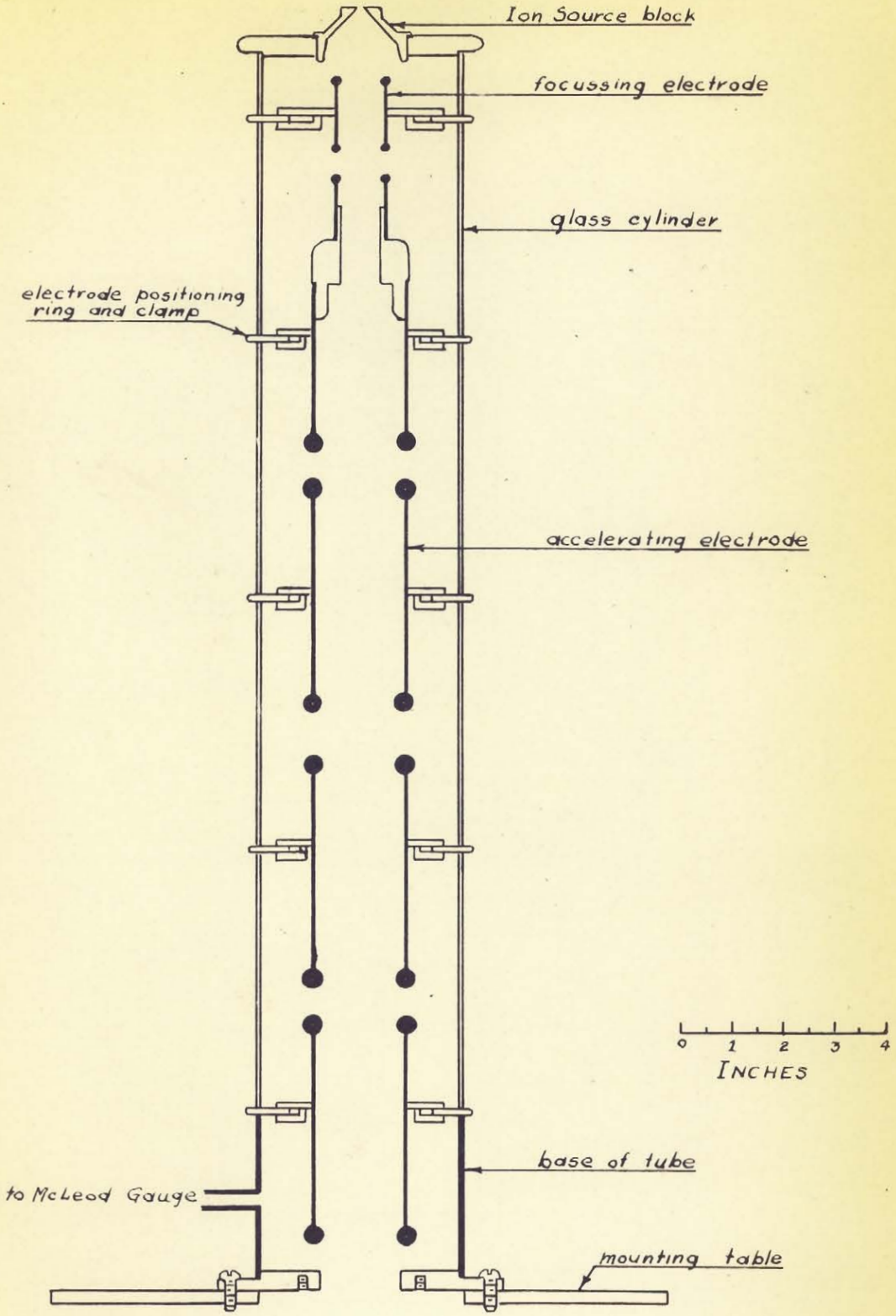

FIG. 5

HIGH VOLTAGE SUPPLY

BLOCK DIAGRAM

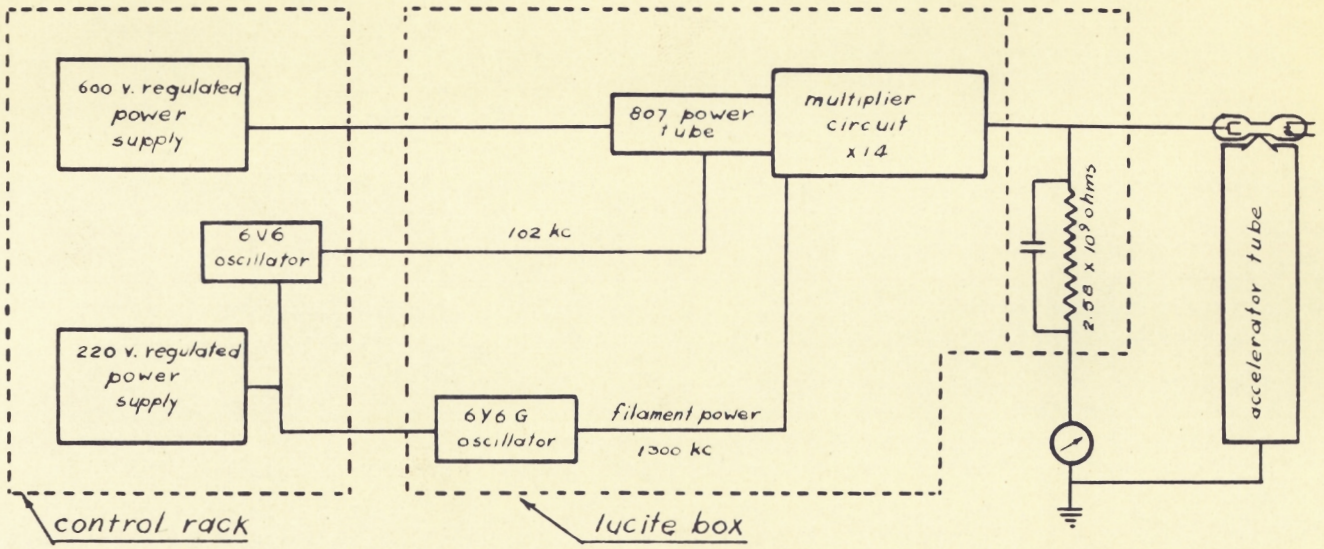

FIG. 6.

600 VOLT REGULATED POWER SUPPLY

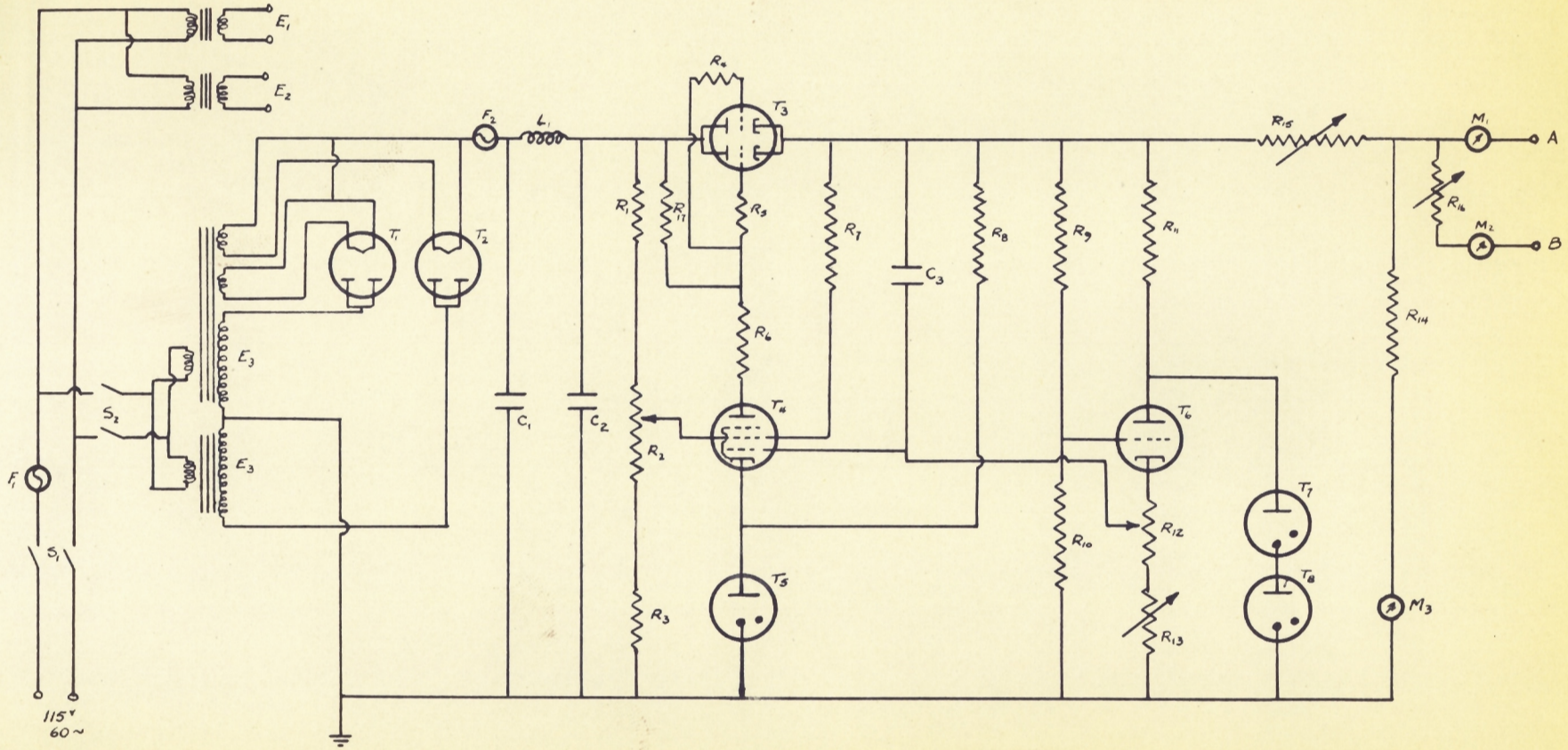

FIG. 7.

CIRCUIT COMPONENTS FOR THE 600 VOLT REGULATED POWER SUPPLY (FIG. 7)

A. - Plate Volts for 807 (Fig. 9)

B. - Screen Volts for 807 (Fig. 9)

R_1 - 100K 4W

R_2 - 20K 2W

R_3 - 80K 4W

R_4 - 100Ω 1W

R_5 - 100Ω 1W

R_6 - 16K 2W

R_7 - 250K 1W

R_8 - 150K 1W

R_9 - 470K 1W

R_{10} - 150K 1W

R_{11} - 15K 10W

R_{12} - 20K 4W

R_{13} - 2K 4W

R_{14} - 600K 1W

R_{15} - Circuit of dropping resistors

R_{16} - 50K 4W

R_{17} - 45K 4W

T_1 - 5U4G

T_2 - 5U4G

T_3 - 6AS7

T_4 - 6SH7

T_5 - VR 150

T_6 - 6J5

T_7 - VR 150

T_8 - VR 150

C_1 - 1 μf 1000 WVDC

C_2 - 8 μf 1000 WVDC

C_3 - 2 μf

M_1 - 100 ma

M_2 - 15 ma

M_3 - 1 ma

E_1 - 6.3^V, 2.5^A (6AS7)

E_2 - 6.3^V, 2.5^A (6J5, 6SH7)

E_3 - 700 volts RMS

S_1 - line switch

S_2 - H.T. switch

F_1 - 2 amp fuse

F_2 - 1/4 amp fuse

6V6 OSCILLATOR

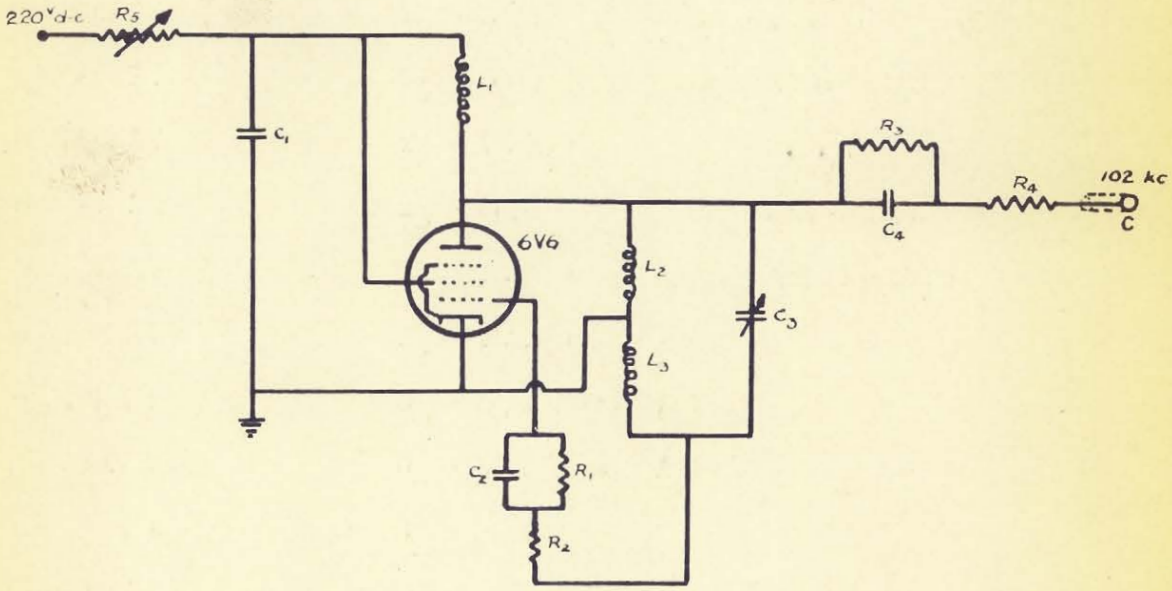

L_1 - 4 mh.
L_2 - 1.1 mh.
L_3 - .25 mh.

C_1 - .05 μf.
C_2 - .05 μf.
C_3 - .0015 μf.
C_4 - .05 μf.

R_1 - 20 kΩ 1 W.
R_2 - 470 Ω 1 W.
R_3 - 12.8 kΩ 2 W.
R_4 - 470 Ω 1 W.
R_5 - 50 kΩ 4 W.

C - To Grid of 807 (Fig. 9)

FIG. 8.

VOLTAGE MULTIPLIER CIRCUIT

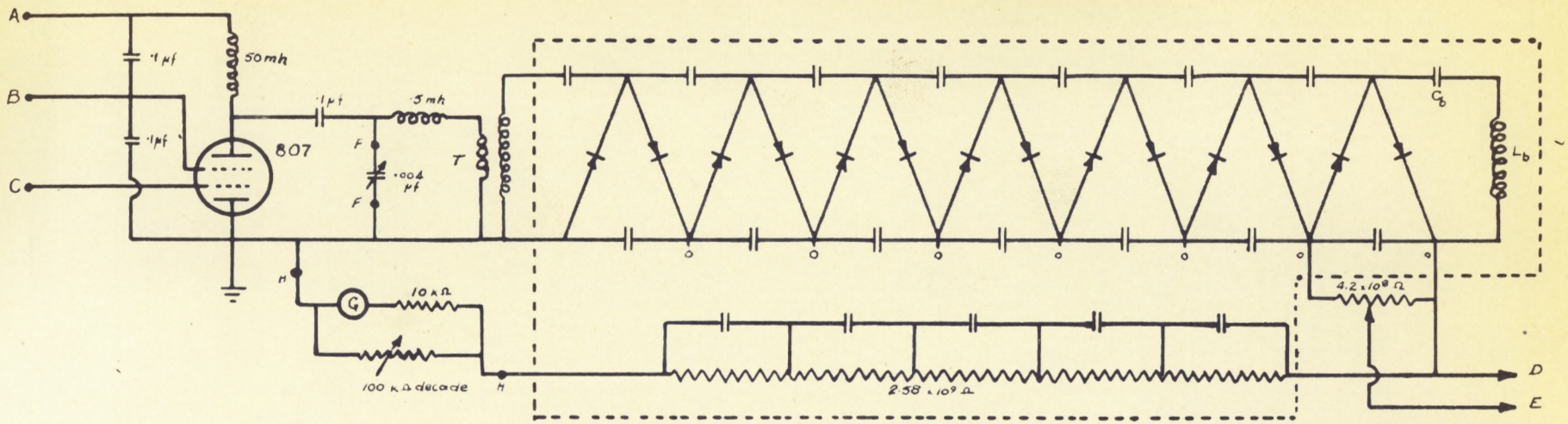

A - Plate volts from 600 volt supply (Fig. 7)
B - Screen volts from 600 volt supply (Fig. 7)
C - R.F. volts from 6V6 oscillator (Fig. 8)
D - To top of Accelerator
E - Focussing volts to first electrode of Accelerator
F - Variable condenser is mounted in control rack and connected to this circuit by co-axial cable
G - Galvanometer; .0038 μa/mm.
H - Connections to control rack
O - d-c output points

All unmarked condensers (and C_b) are .001 μf 20,000 wvdc
All unmarked rectifiers are 1B3/8016 diodes
Components inside dotted line are oil immersed except for tops of rectifiers

FIG. 9.

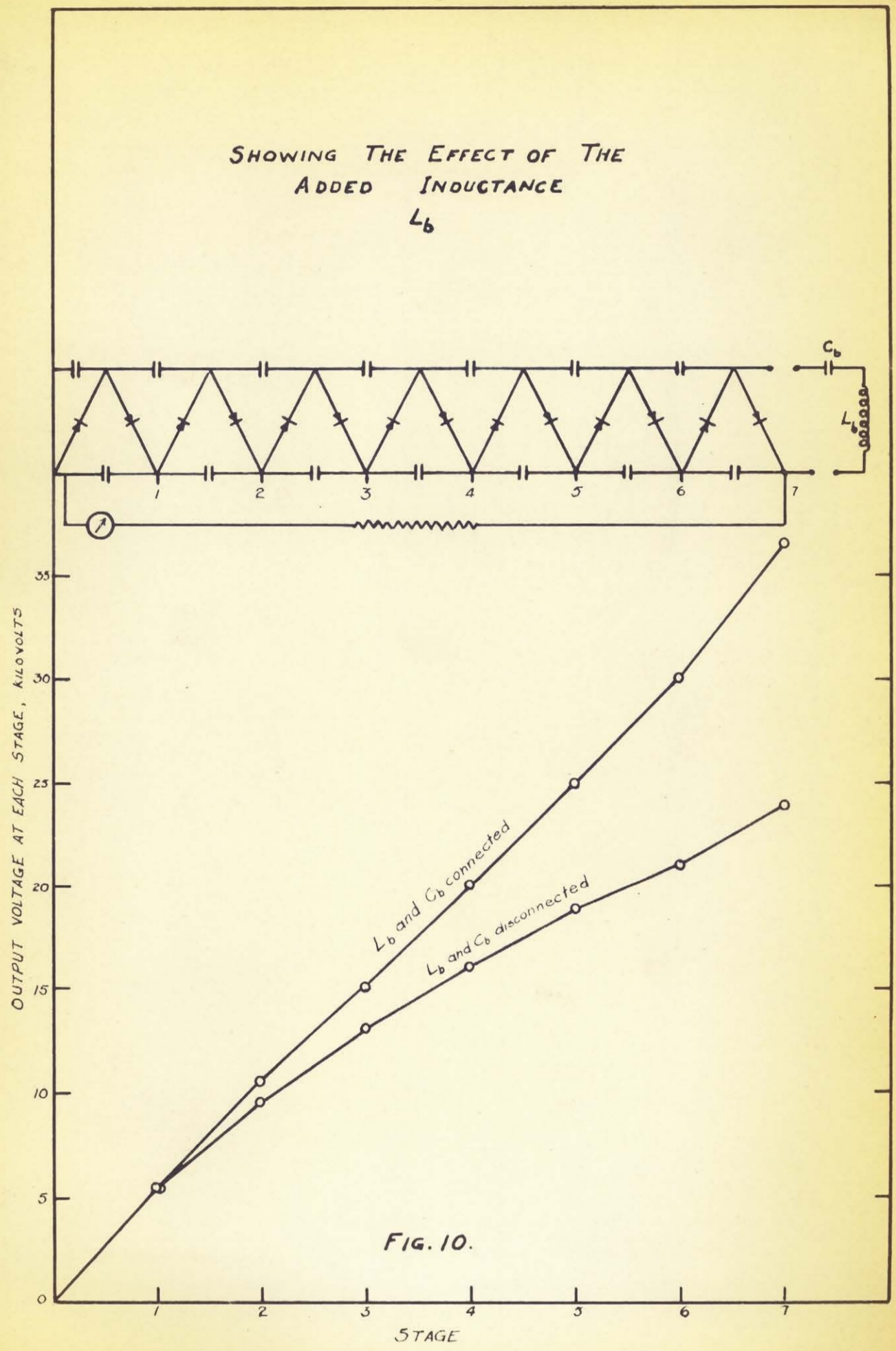
SHOWING THE EFFECT OF THE
ADDED INDUCTANCE
L_b
C_b
L_b
1
2
3
4
5
6
7
OUTPUT VOLTAGE AT EACH STAGE, KILOVOLTS
0
5
10
15
20
25
30
35
L_b and C_b connected
L_b and C_b disconnected
STAGE

FIG. 10.

DIODE FILAMENT CIRCUIT

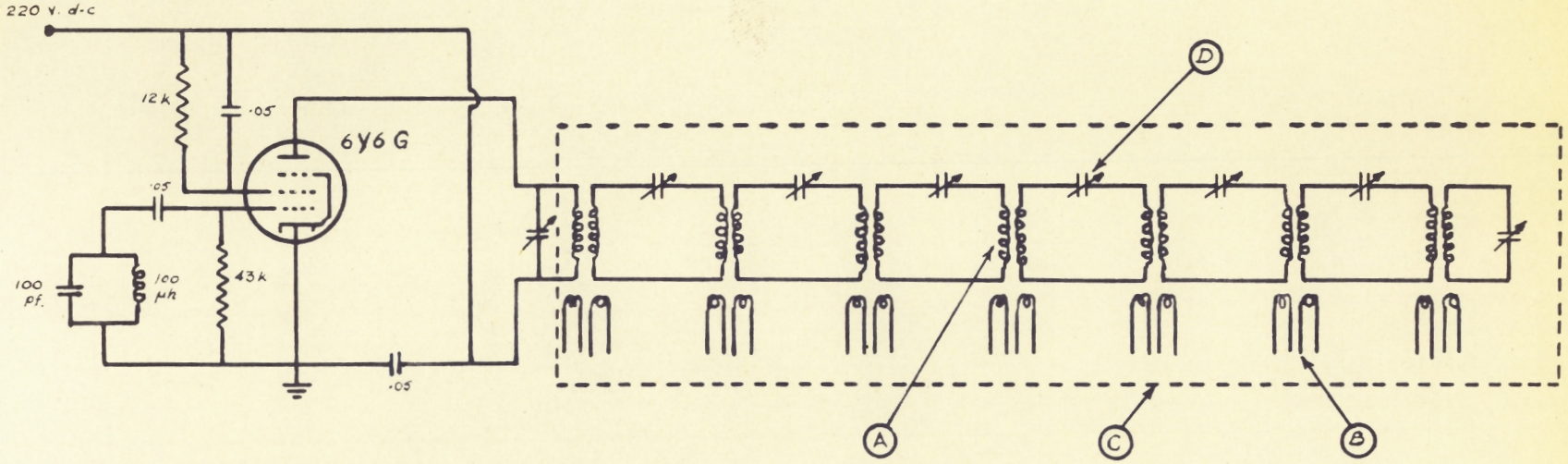

(A) R-F isolating transformers. Both primary and secondary inductances 240 μh.

(B) Pick-up loops connected to filaments of 1B3/3016 diodes in voltage-multiplier circuit.

(C) Components within dotted line are oil-immersed.

(D) Tuning Condensers, 140 μμf.

Operating frequency 1300 kc.

FIG. 11.

EXPERIMENTAL ATTACHMENTS

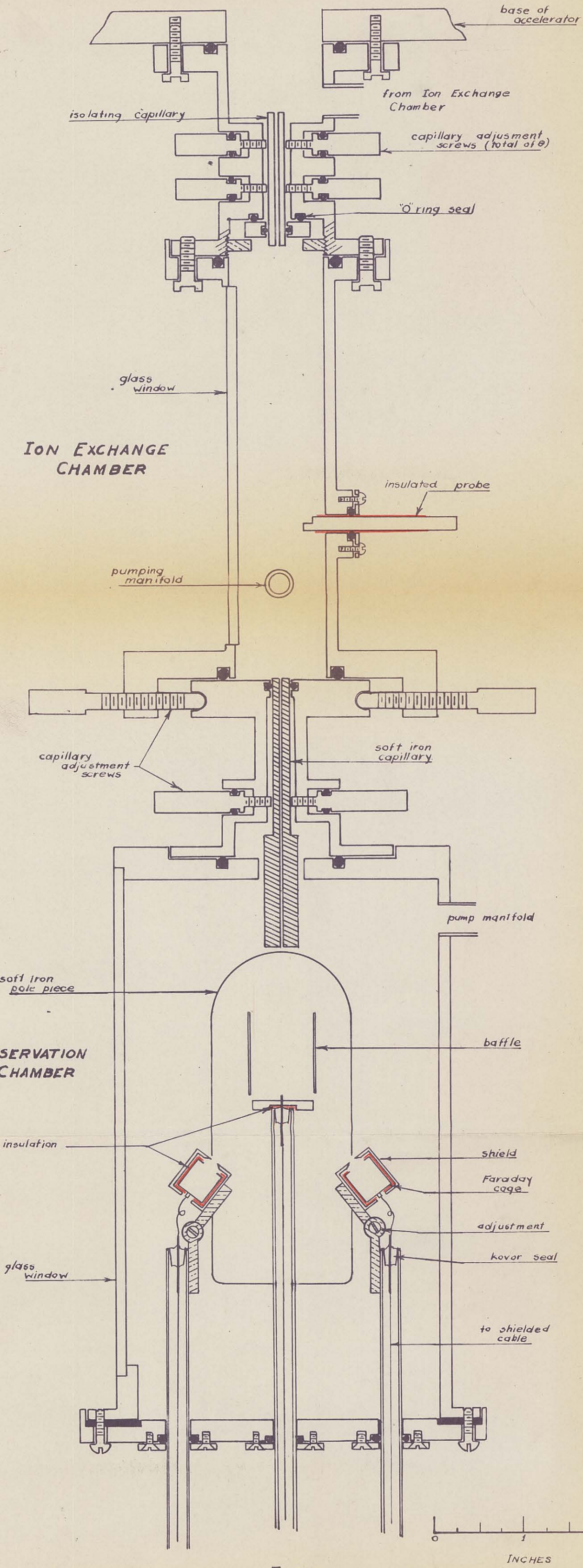

FIG. 12

RATIO RESISTANCE CIRCUIT

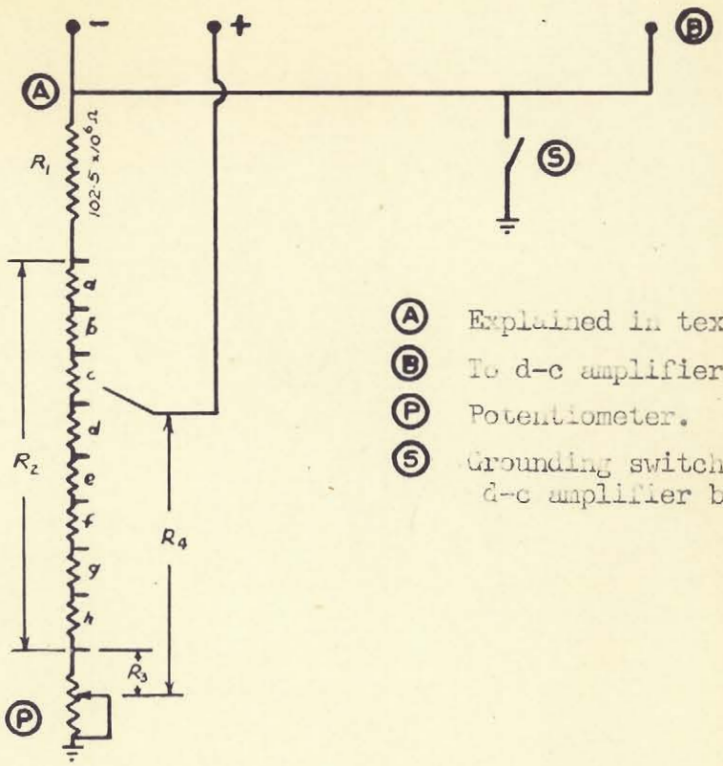

One set of resistances making up R_2 and R_3 was not sufficient for the accurate measurement of (i^-/i^+) over the whole range observed.

Thus for values of $(i^-/i^+)_c$ from 0 to 4 percent, R_2 and P had the values shown under I below; and for $(i^-/i^+)_c$ from 3 to 24 percent, R_2 and P had values listed under II.

I		II	
a =	$1.00 \times 10^6\ \Omega$	a =	$2.72 \times 10^6\ \Omega$
b =	1.09	b =	3.07
c =	1.11	c =	2.92
d to h =	.00	d =	2.93
Total =		e =	2.93
R_2 =	3.20	f =	3.02
P =	$1 \times 10^6\ \Omega$	g =	2.94
		h =	3.46
		Total = R_2 =	$24.00 \times 10^6\ \Omega$
		P =	$4 \times 10^6\ \Omega$

FIG. 13.

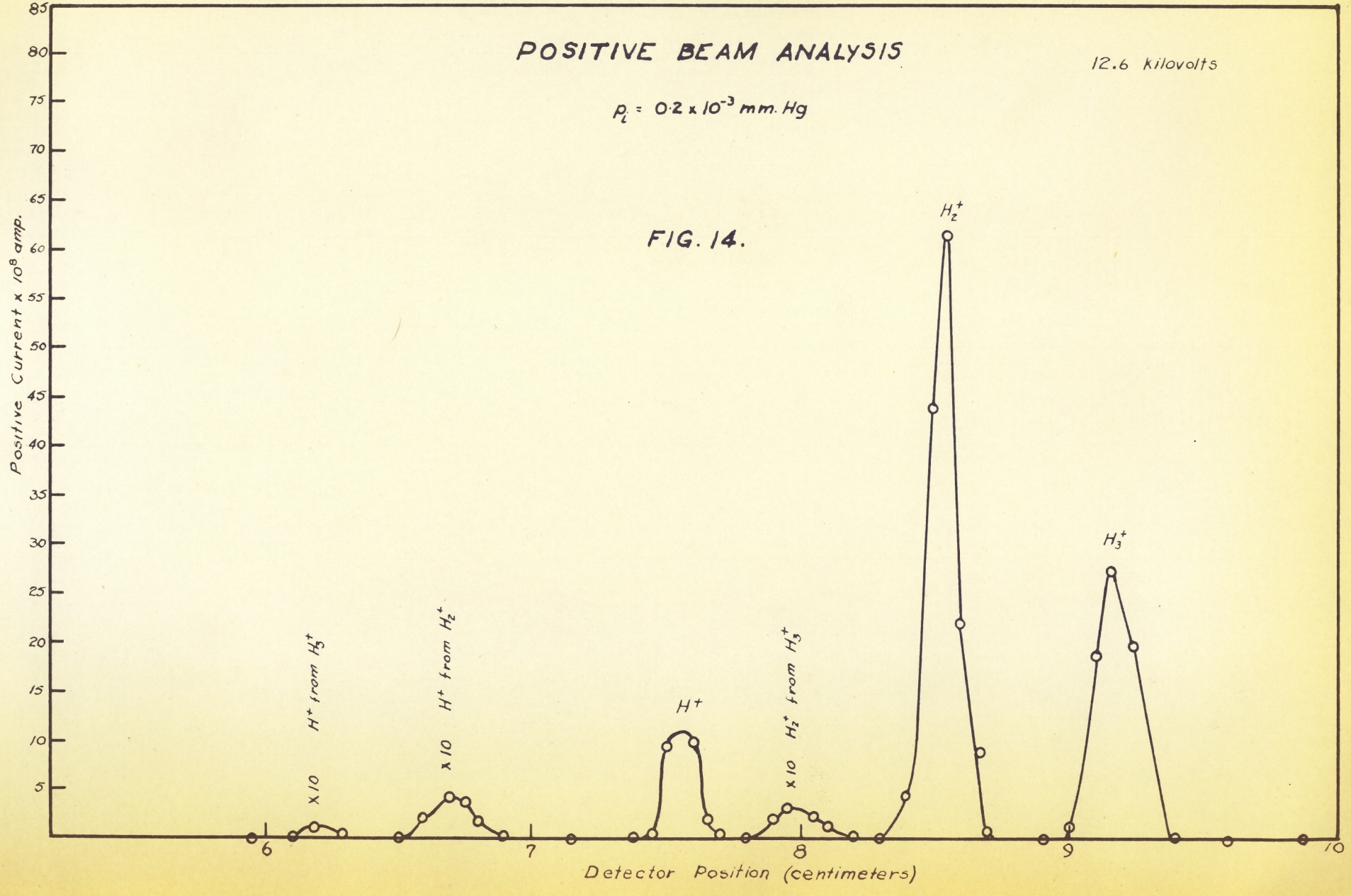
POSITIVE BEAM ANALYSIS
12.6 kilovolts
$p_i = 0.2 \times 10^{-3}$ mm. Hg
FIG. 14.
Positive Current x 10^8 amp.
Detector Position (centimeters)
H^+ from H_3^+
x 10
H^+ from H_2^+
x 10
H^+
H_2^+ from H_3^+
x 10
H_2^+
H_3^+

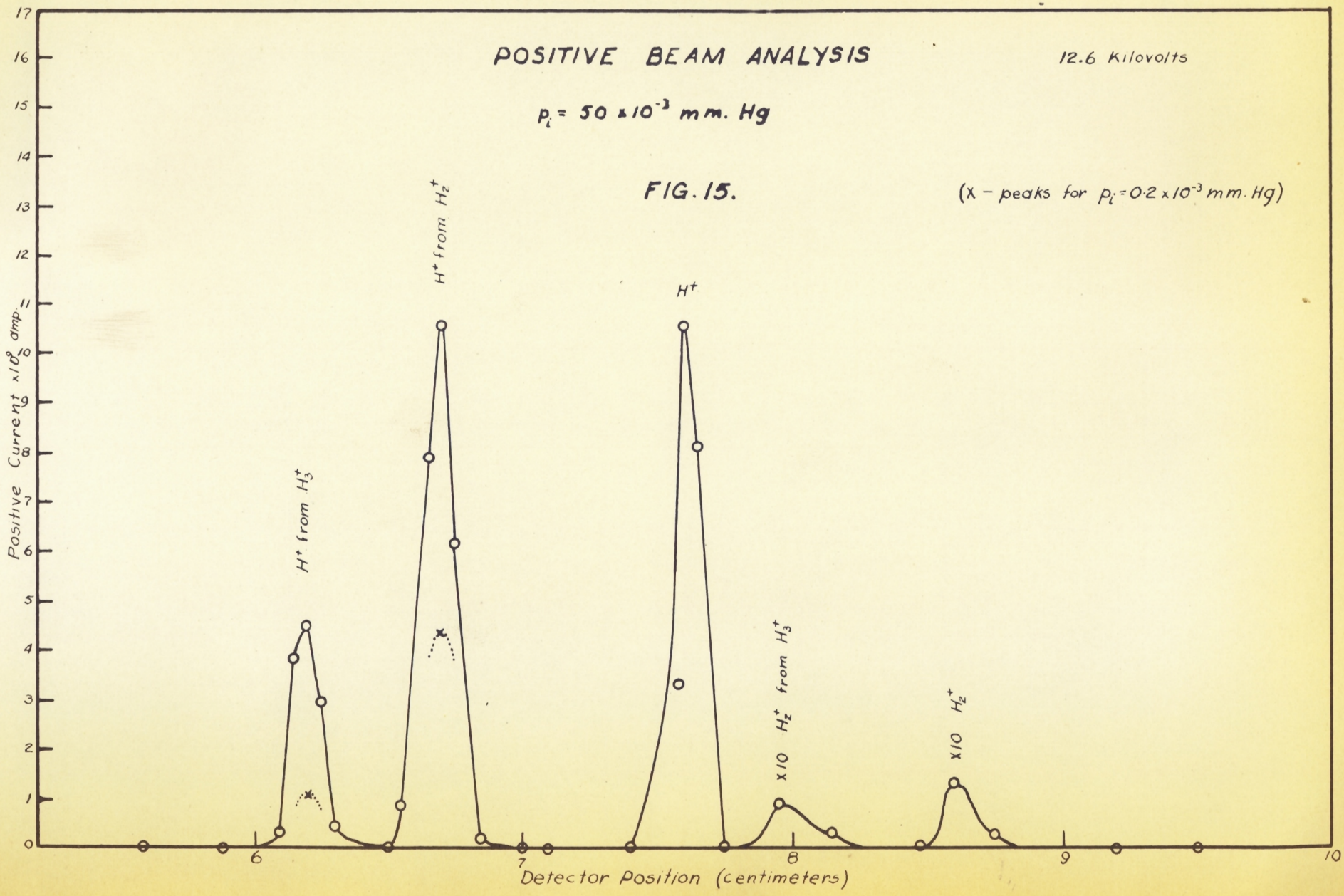
POSITIVE BEAM ANALYSIS
12.6 Kilovolts
$p_i = 50 \times 10^{-3}$ mm. Hg
FIG. 15.
(X – peaks for $p_i = 0.2 \times 10^{-3}$ mm. Hg)
Positive Current $\times 10^{-9}$ amp.
Detector Position (centimeters)
H^+ from H_3^+
H^+ from H_2^+
H^+
x10 H_2^+ from H_3^+
x10 H_2^+

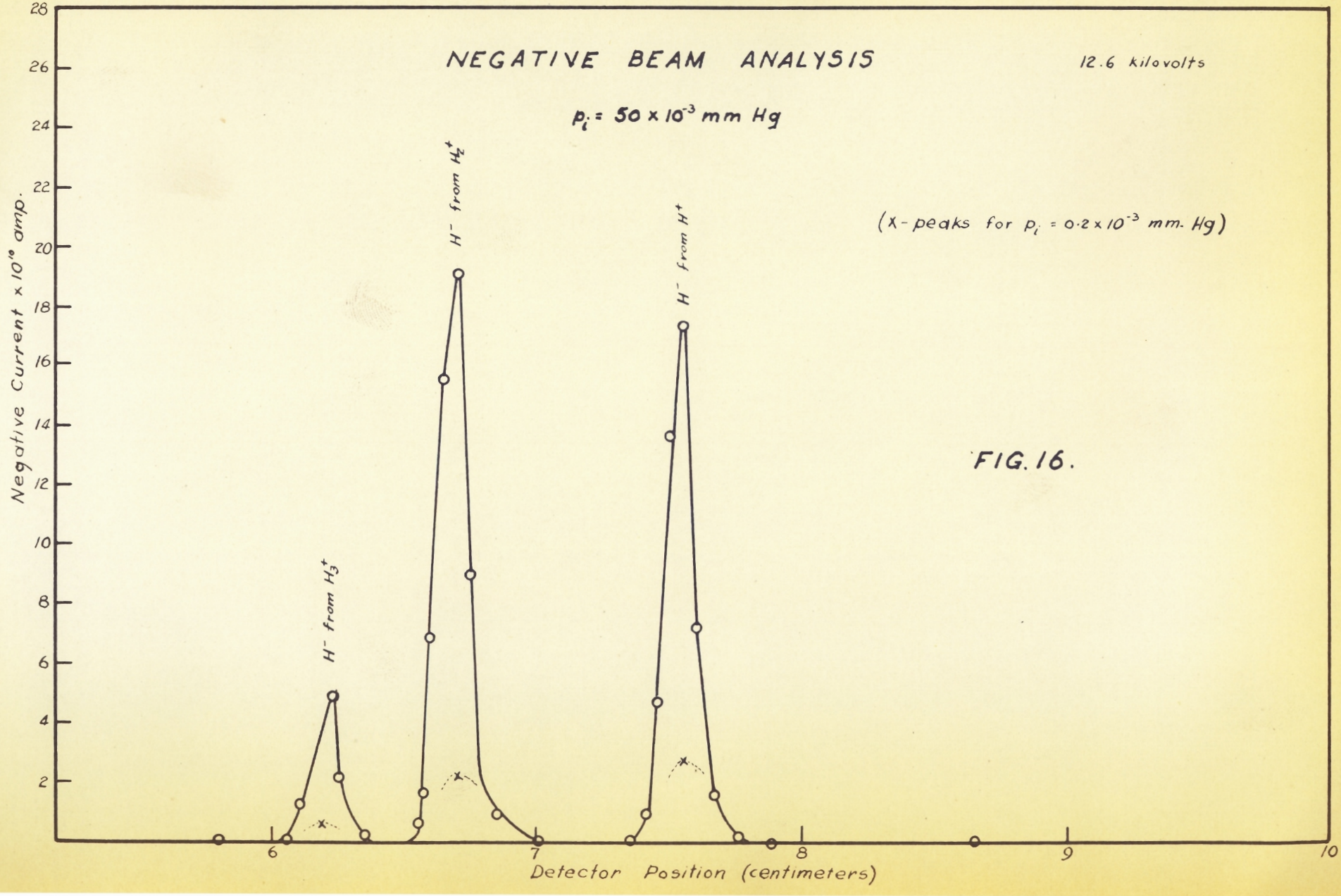
NEGATIVE BEAM ANALYSIS
12.6 kilovolts
$p_i = 50 \times 10^{-3}$ mm Hg
(X-peaks for $p_i = 0.2 \times 10^{-3}$ mm. Hg)
H^- from H_3^+
H^- from H_2^+
H^- from H^+
Negative Current $\times 10^{10}$ amp.
Detector Position (centimeters)
28
26
24
22
20
18
16
14
12
10
8
6
4
2
6
7
8
9
10

FIG. 16.

THE VARIATION OF i^-/i^+ WITH p_i
12.6 KV.

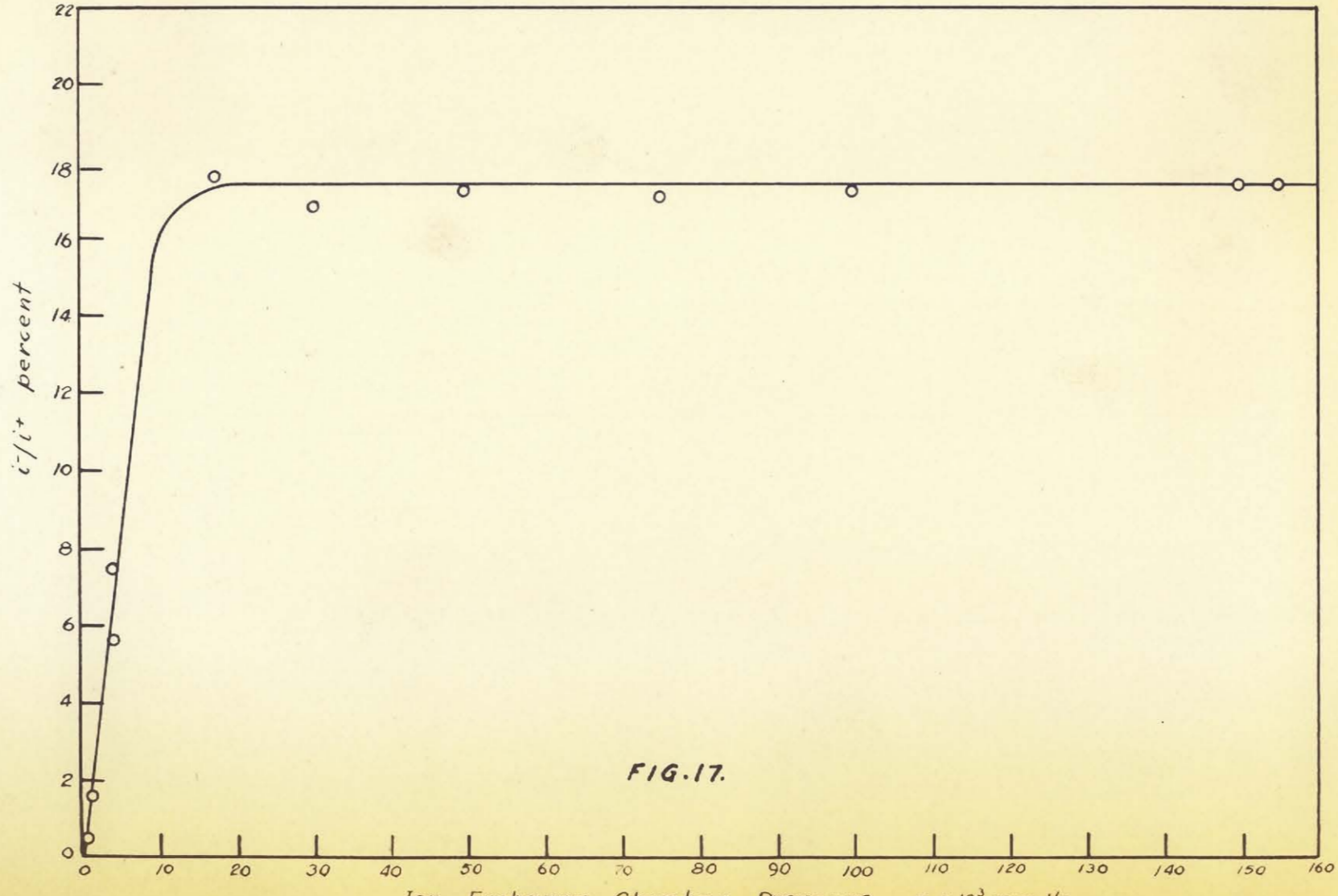

FIG. 17.

THE VARIATION OF i^- WITH P_i
12.6 KV.

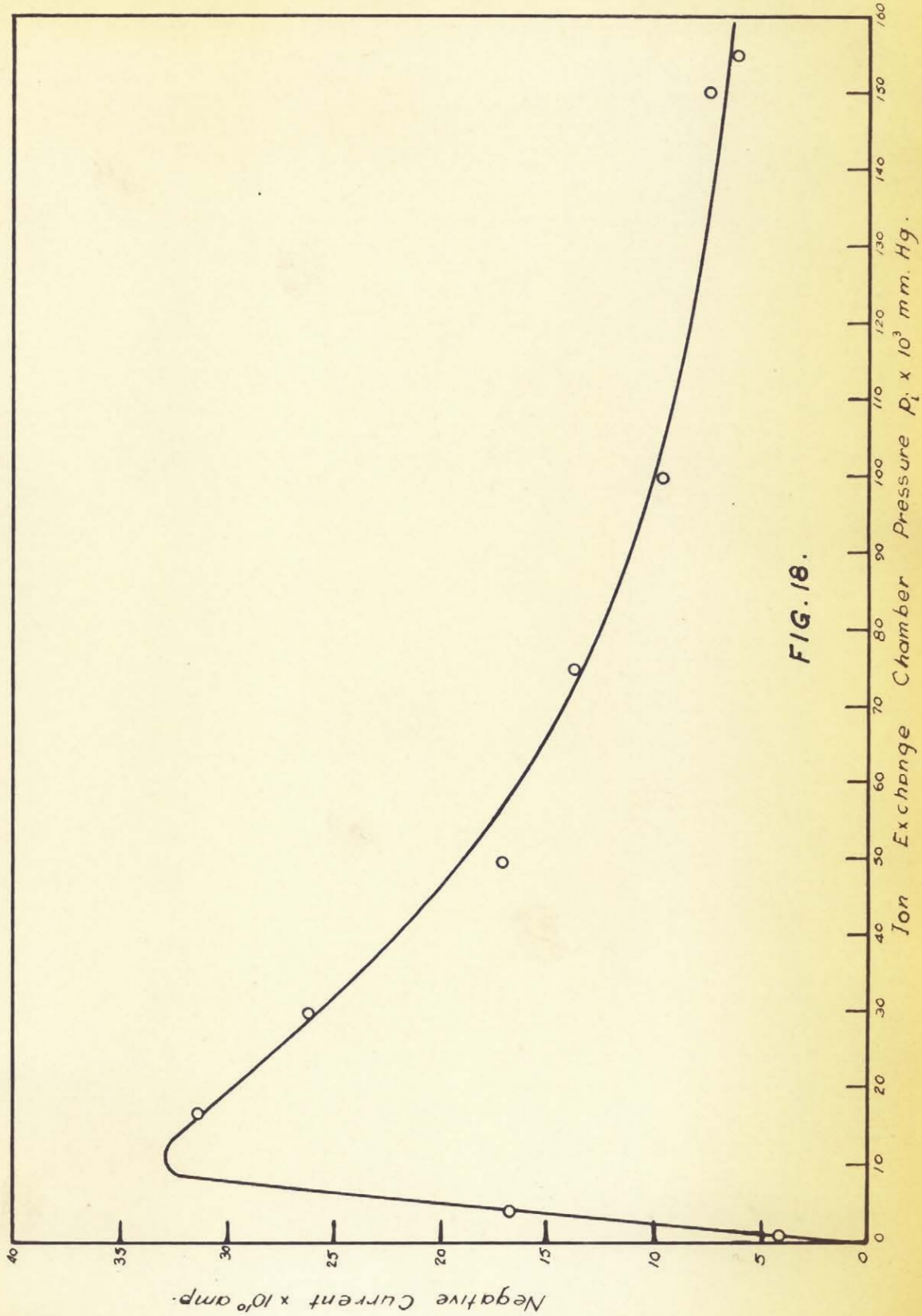

FIG. 18.

THE VARIATION OF i^+ WITH p_i

12.6 KV.

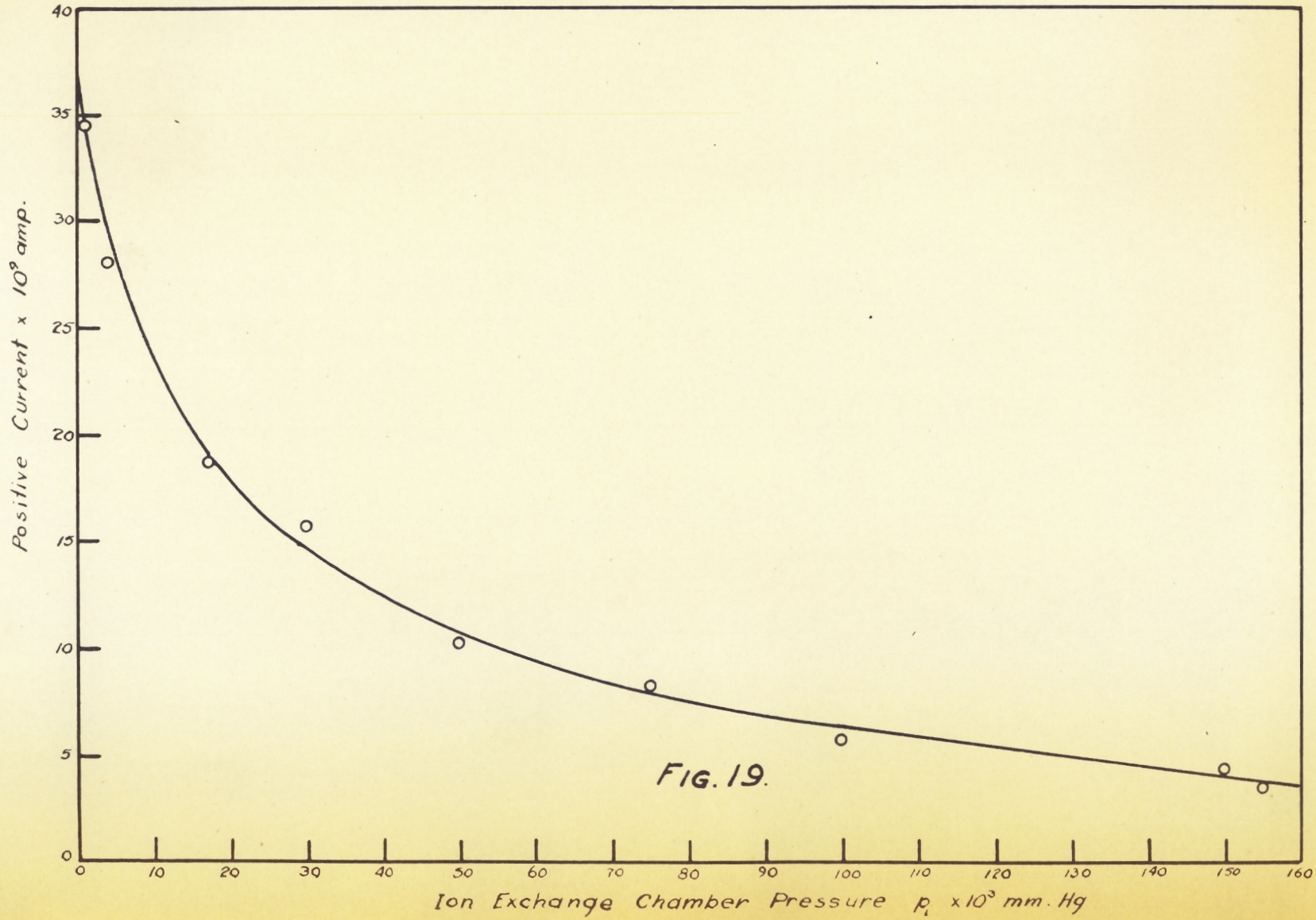

FIG. 19.

MULTIPLE CHARGE EXCHANGE

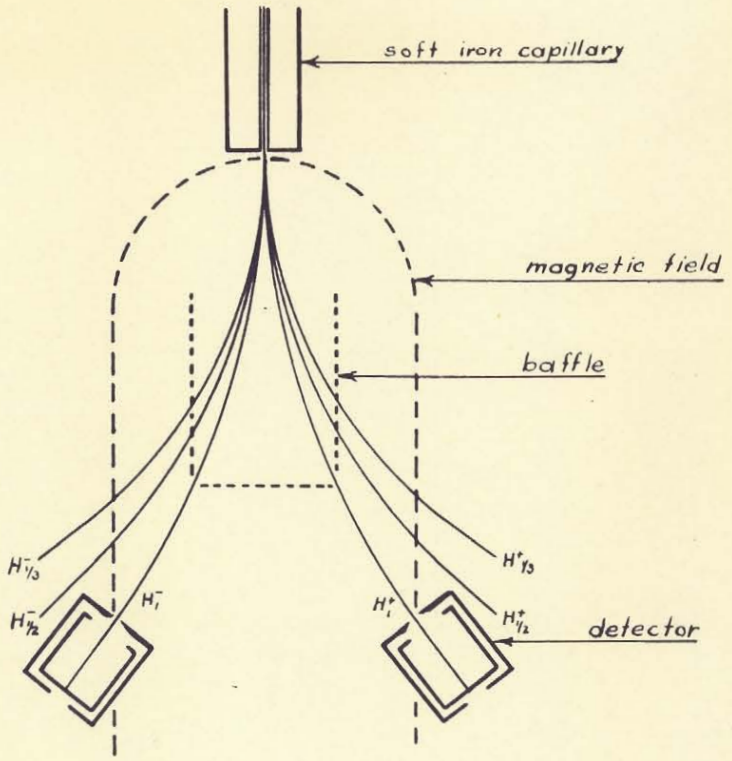

FIG. 20

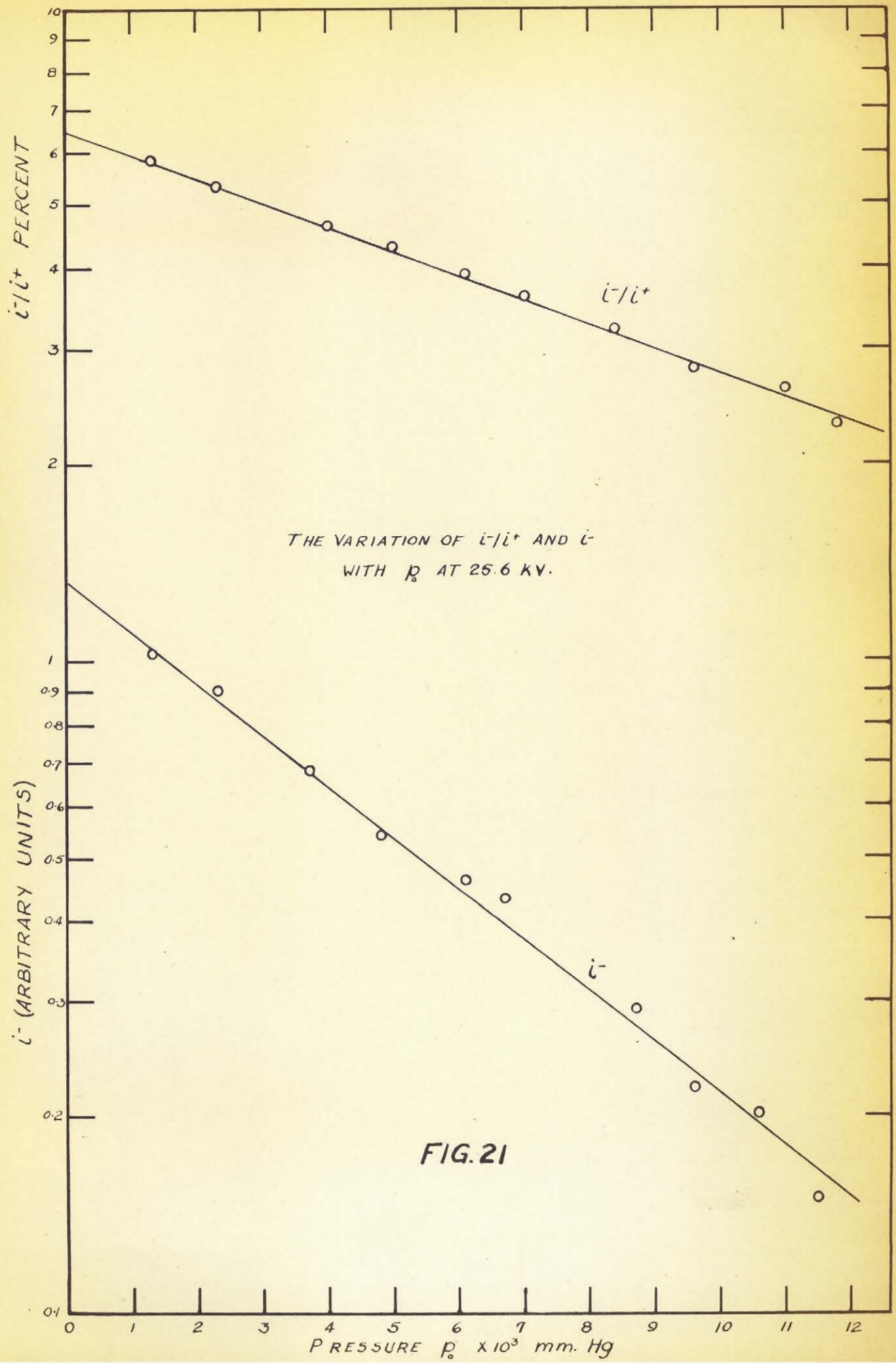
i⁻/i⁺ PERCENT
i⁻/i⁺
THE VARIATION OF i⁻/i⁺ AND i⁻
WITH p₀ AT 25.6 KV.
i⁻ (ARBITRARY UNITS)
i⁻
PRESSURE p₀ X 10³ mm. Hg

FIG. 21

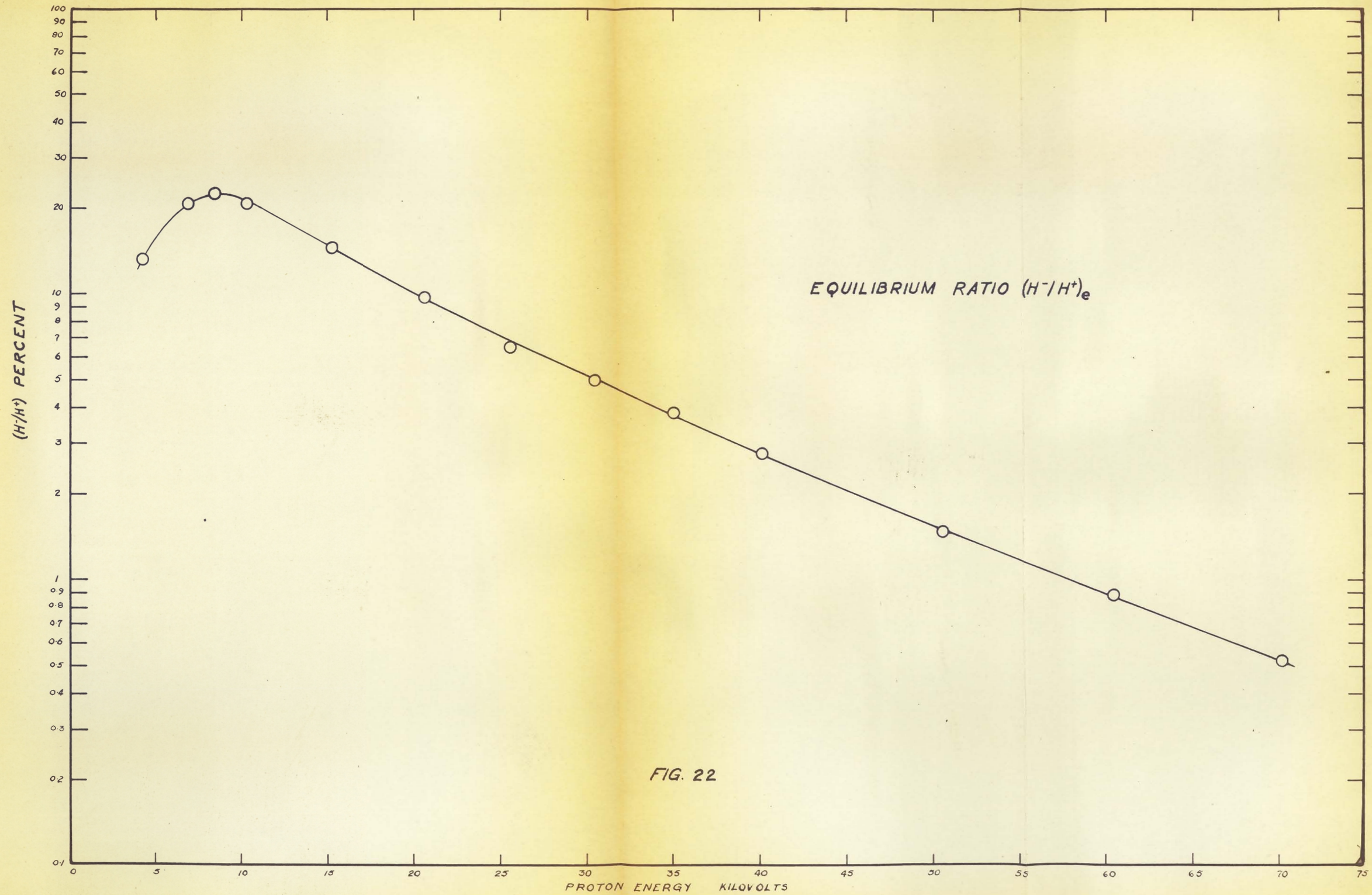
EQUILIBRIUM RATIO $(H^-/H^+)_e$
(H^-/H^+) PERCENT
100
90
80
70
60
50
40
30
20
10
9
8
7
6
5
4
3
2
1
0.9
0.8
0.7
0.6
0.5
0.4
0.3
0.2
0.1
0
5
10
15
20
25
30
35
40
45
50
55
60
65
70
75
PROTON ENERGY KILOVOLTS

FIG. 22

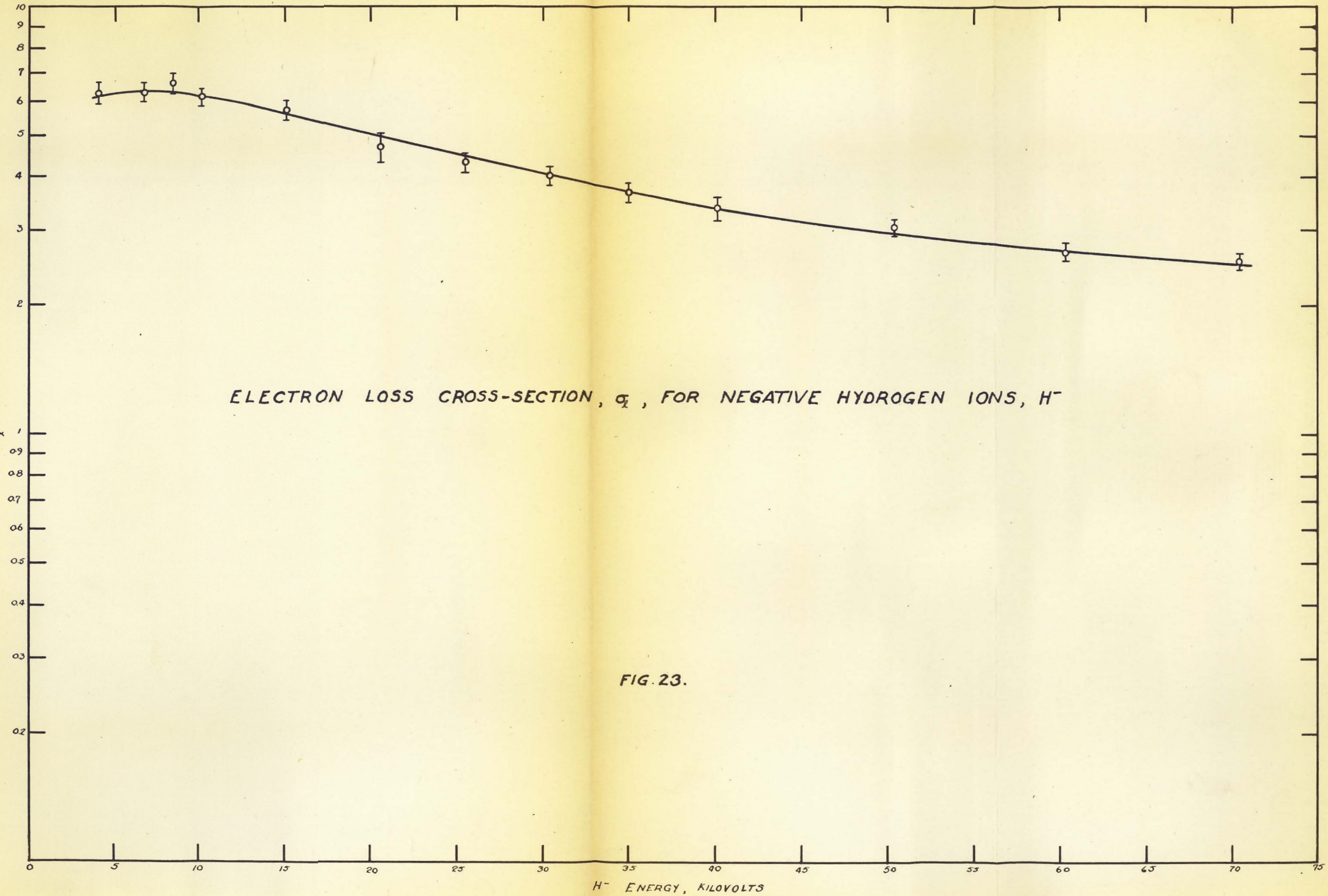
ELECTRON LOSS CROSS-SECTION, σ_l, FOR NEGATIVE HYDROGEN IONS, H^-
$\sigma_l \times 10^{16}$ cm²
10
9
8
7
6
5
4
3
2
1
0.9
0.8
0.7
0.6
0.5
0.4
0.3
0.2
0
5
10
15
20
25
30
35
40
45
50
55
60
65
70
75
H^- ENERGY, KILOVOLTS

FIG. 23.

ELECTRON CAPTURE CROSS-SECTION, σ_c, FOR NEUTRAL HYDROGEN ATOMS, H°

$\sigma_c = \left(\frac{\sigma_i'}{\sigma_i}\right)\left(\frac{H^-}{H^+}\right)_e \sigma_i$

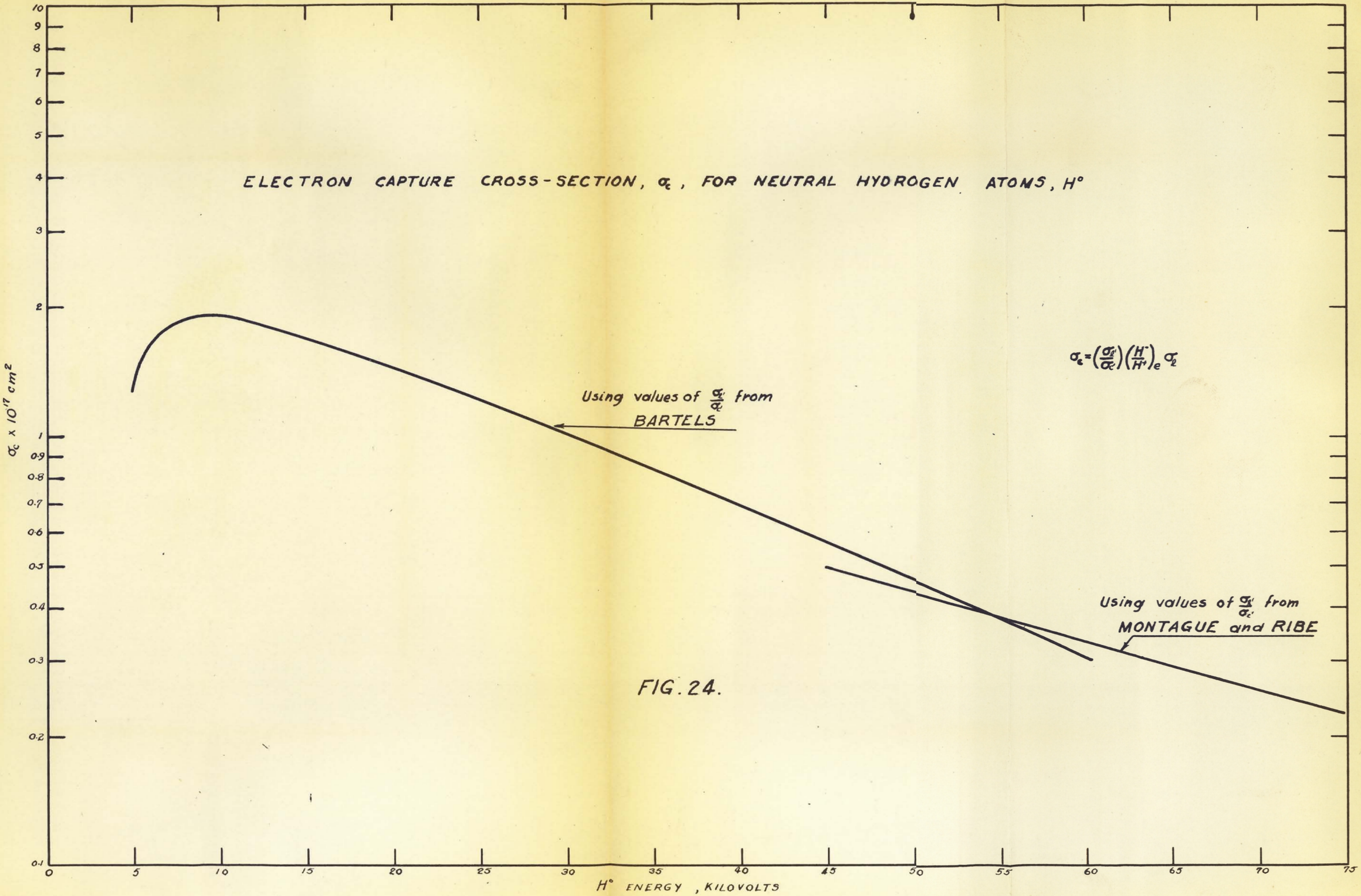

FIG. 24.

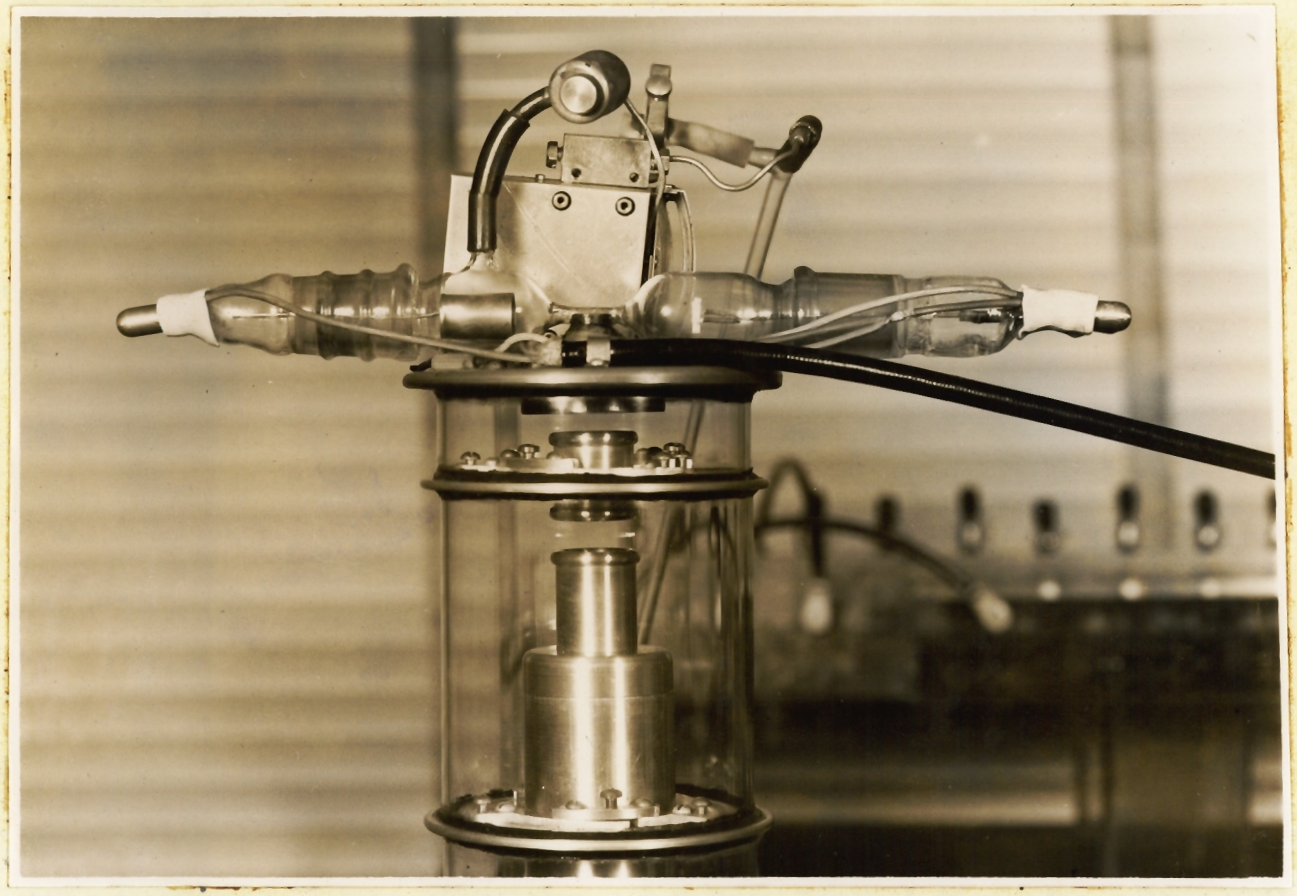

PLATE I. Ion Source. The anode is to the left of the capillary, the filament to the right. The lower end of the copper focussing cone can be seen just below the brass plate at the top of the accelerator column. Also shown are the first and second focussing electrodes of the accelerator.

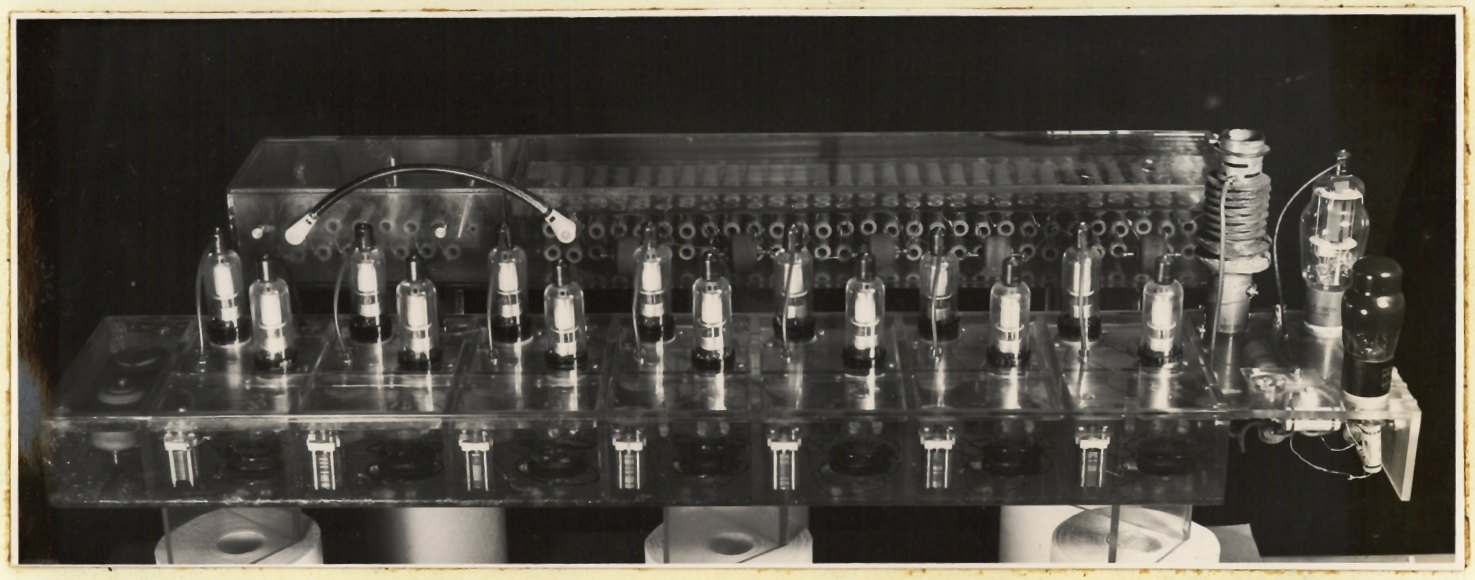

PLATE II. High Voltage Supply. The 807 power tube and R-F transformer can be seen to the right rear. The 6Y6G oscillator tube which supplies power to the diode filaments is at the right front. The fourteen diodes can be seen protruding through the top of the lucite box. Inside the box, in the foreground, R-F isolating transformers and tuning condensers for the filament heater circuit are visible. The lucite box in the background contains the bleeder resistor in the large section to the right, and the focussing voltage resistors in the small section to the left.

PLATE III. High Voltage Supply. The added inductance, L_b, can be seen at the far right. The seven d-c output terminals are visible along the near side of the lucite box in the foreground. Also in the foreground, inside the box, can be seen seven of the fourteen condensers of the voltage multiplier circuit.

PLATE IV. Experimental Chambers. The base of the accelerator can be seen at the top of the picture. In descending order are shown the housing and adjustment for the top capillary, the Ion Exchange Chamber, the housing and adjustment for the soft iron capillary, the Observation Chamber and magnets, and the three shafts to which are attached the two detectors and the centre baffle. Part of one detector can be seen through the window of the Observation Chamber

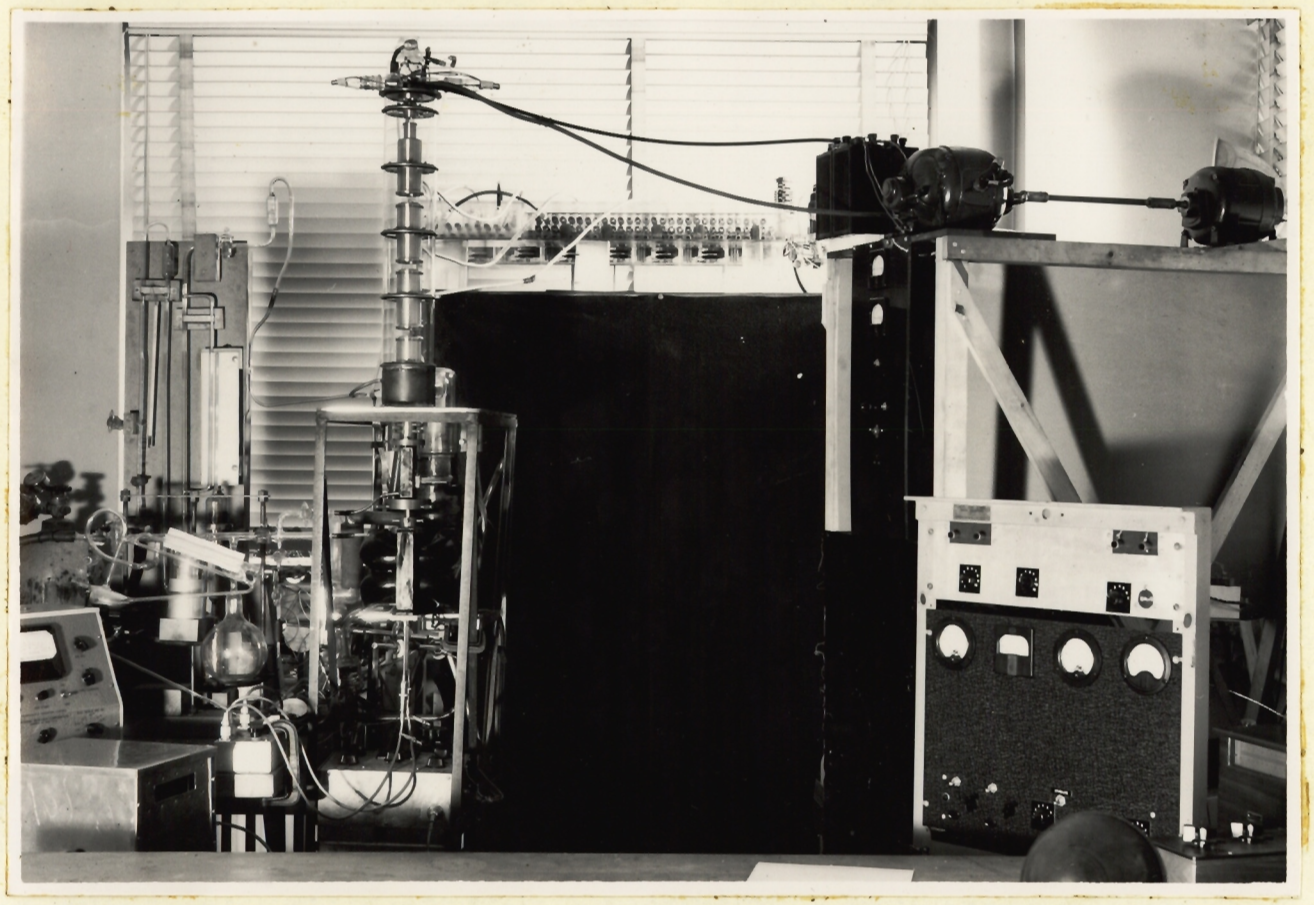

PLATE V. General View of Equipment. The accelerator and experimental chambers are shown to the left of centre. In the lower left corner can be seen the gas handling system for the Ion Exchange Chamber, the Ratio Resistance Circuit, the ionization gauge, and the shielded galvanometer for the d-c amplifier. To the right of the accelerator are the high voltage supply, and the motor-generator for the ion source. The control rack and galvanometer for high voltage measurement can be seen at the lower right corner of the photograph.